

Figure S1

Gating strategy for H3.3K27M-reactive CD8+ T-cells. A representative gating strategy to identify CD8+ T-cells from patient-derived PBMCs that exhibit reactivity for K27M on CyTOF above background levels. Cells staining double-positive with iridium (Ir) intercalator in channels 191 and 193 were identified as intact cells (*left*). Cells with low cisplatin staining were identified as live cells (*second to left*). Cells staining positive for CD45 and CD3 were selected as T-cells (*middle*). Cells staining positive for CD8+ were identified as CD8+ T-cells (*second to right*). Cells staining above background levels with H3.3K27M dextramer were identified as H3.3K27M-reactive CD8+ T-cells (*right*). Healthy donor (**A**) and H3.3K27M-specific TCR-transduced CD8+ T-cells (**B**) were used to validate the specificity and sensitivity of the H3.3K27M dextramer respectively. CD8+ T-cells derived from a representative patient (**C**) exhibiting reactivity for H3.3K27M above background were classified as H3.3K27M-reactive CD8+ T-cells.

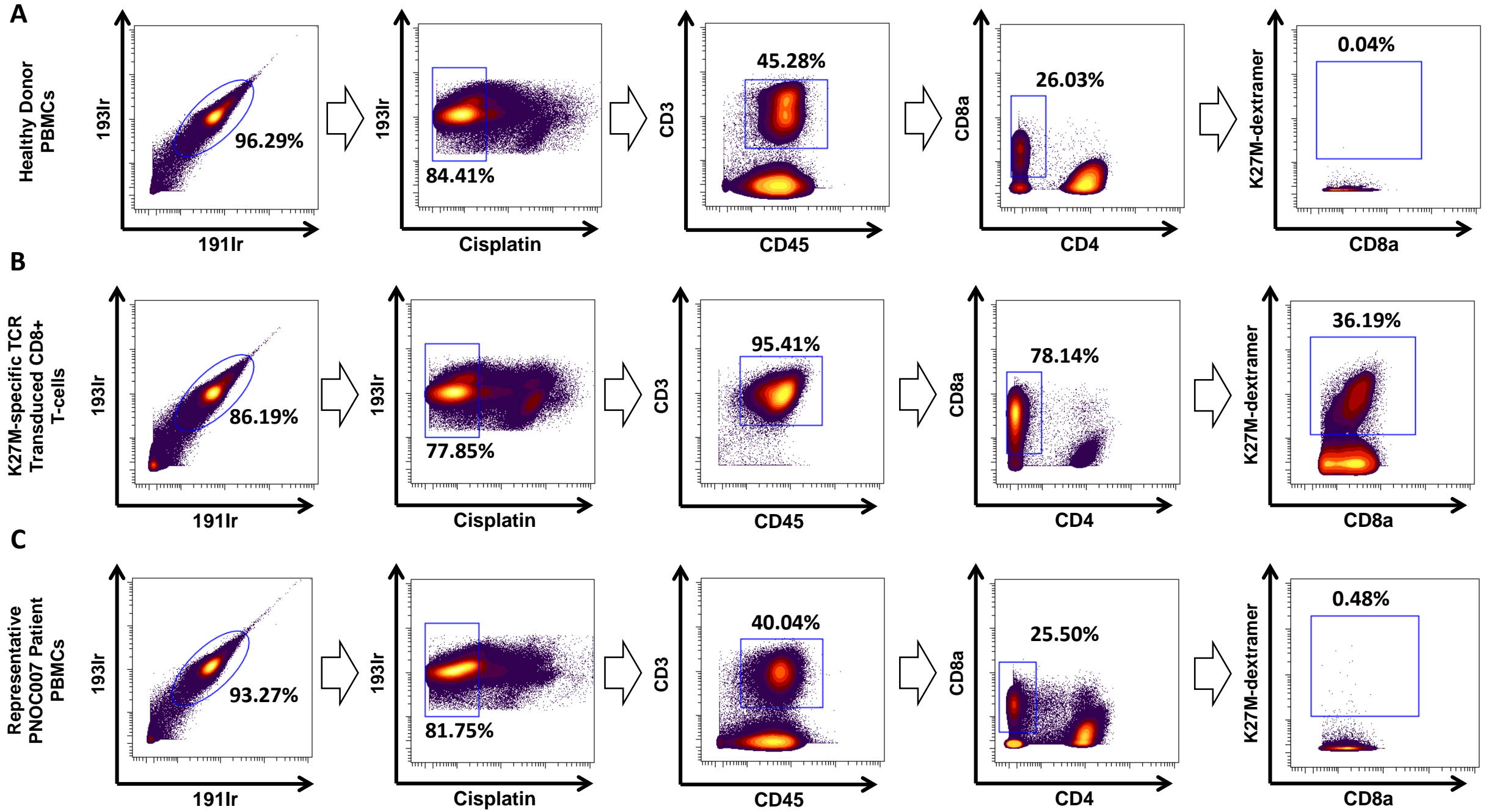


Figure S2

Mass cytometry-based detection of H3.3K27M-reactive CD8+ T-cell is as sensitive as conventional flow cytometry using H3.3K27M dextramer. CD8+ T-cells were detected from the same patient on both flow cytometry (*above*) and mass cytometry (*below*), exhibiting comparable percentages of overall CD8+ T-cells that were identified as H3.3K27M-reactive.

PNOC007-12 CD8+ T-cells

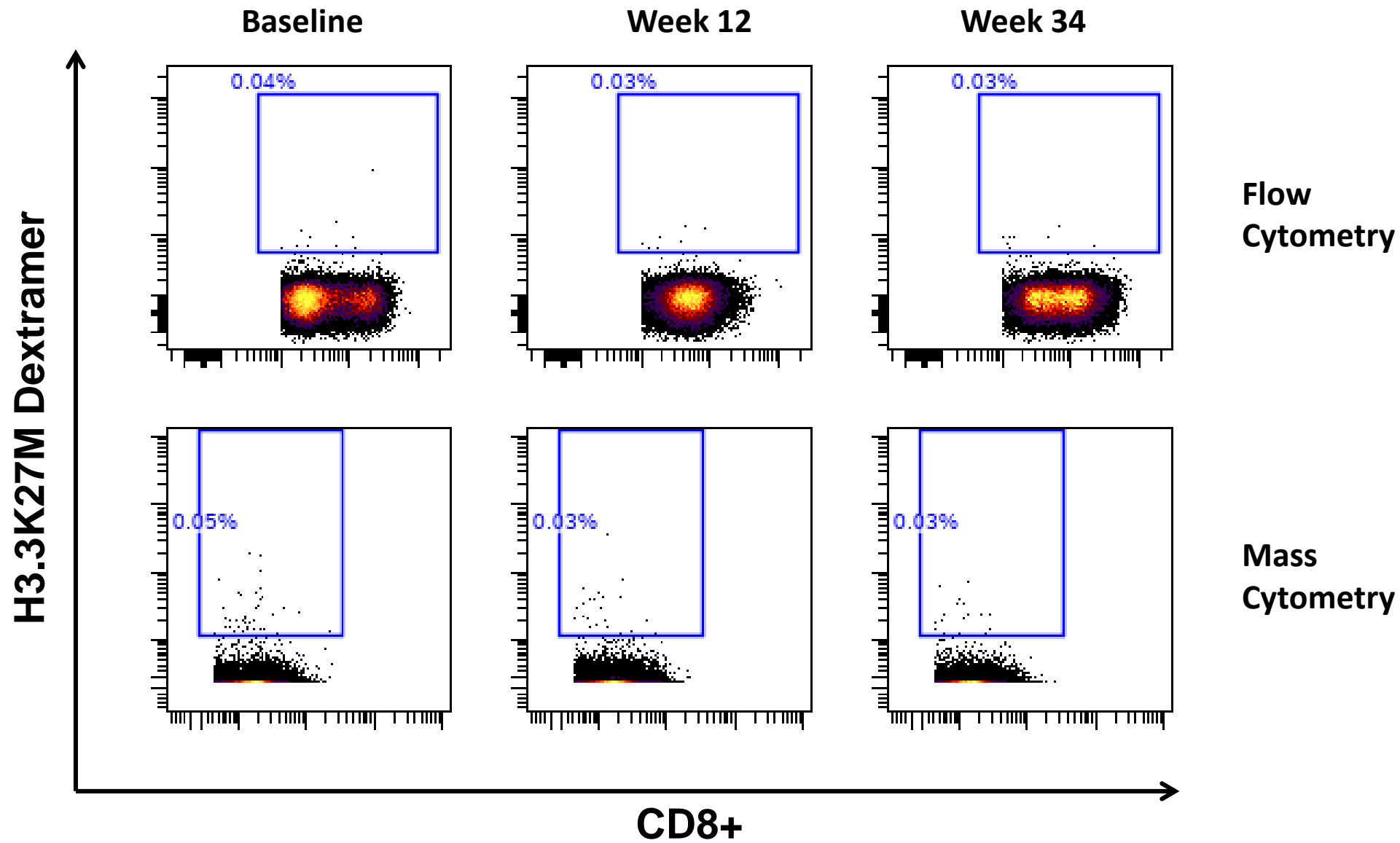
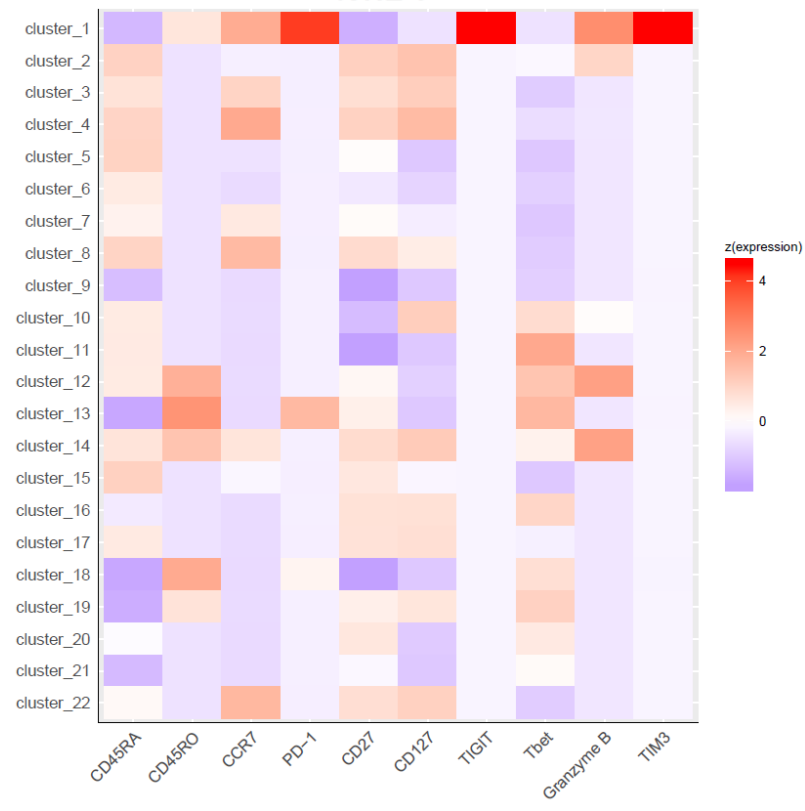
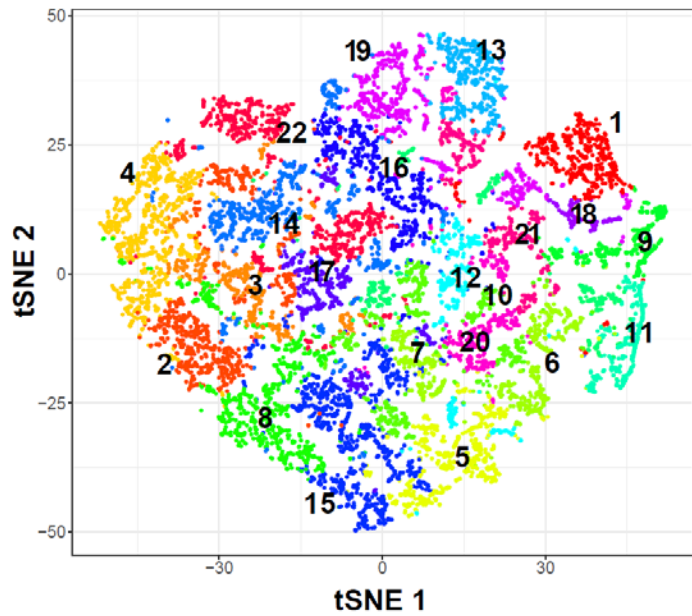


Figure S3

tSNE stratification and expression profiles of discrete H3.3K27M-reactive CD8+ T-cell subpopulations. *Top-left*, H3.3K27M-reactive CD8+ T-cells were stratified on a tSNE plot using the CD8+ T-cell canonical markers: CD45RA, CD45RO, CCR7, CD27, and CD127. *Bottom-left*, heat map visualizing the z-score normalized expression of resultant H3.3K27M-reactive CD8+ T-cell clusters. *Right*, CyTOF-based marker expression profiles and phenotypic characterizations of H3.3K27M-reactive CD8+ T-cell clusters identified via tSNE stratification.



Cluster Number	Phenotype
1	CD45RO ⁺ CD27 ⁻ CD127 ⁻ TIM3 ⁺ PD-1 ⁺ Tbet ⁻
2	CD45RA ⁺ CCR7 ^{lo} CD27 ⁺ CD127 ⁺ CD29 ⁻ Tbet ⁻
3	CD45RA ⁺ CCR7 ⁺ CD27 ⁺ CD127 ⁺ CD29 ⁻ Tbet ⁻
4	CD45RA ⁺ CCR7 ⁺ CD27 ⁺ CD127 ⁺ CD29 ⁻ Tbet ⁻
5	CD45RA ⁺ CCR7 ⁻ CD27 ^{mid} CD127 ⁻ CD29 ⁻ Tbet ⁻
6	CD45RA ⁺ CCR7 ⁻ CD27 ⁻ CD127 ⁻ CD29 ⁻ Tbet ⁻
7	CD45RA ⁺ CCR7 ^{hi} CD27 ^{mid} CD127 ⁻ CD29 ⁻ Tbet ⁻
8	CD45RA ⁺ CCR7 ⁺⁺ CD27 ⁺ CD127 ⁺ CD29 ⁻ Tbet ⁻
9	All markers low
10	CD45RA ⁺ CCR7 ⁻ CD27 ⁻ CD127 ⁺ CD29 ^{hi} Tbet ⁺ CD49d ⁺
11	CD45RA ⁺ CCR7 ⁻ CD27 ⁻ CD127 ⁻ CD29 ^{hi} Tbet ⁺ CD49d ⁻
12	CD45RA ⁺ CD45RO ⁺ CCR7 ^{mid} CD27 ^{hi} CD127 ⁺ CD29 ⁺ Tbet ⁺ CD49d ^{mid}
13	CD45RO ⁺ CCR7 ⁻ CD27 ^{hi} CD127 ⁻ CD29 ⁺ Tbet ⁺
14	CD45RA ⁺ CD45RO ⁺ CCR7 ⁺ CD27 ⁺ CD127 ⁺ CD29 ⁺ Tbet ^{hi} CD49d ⁺
15	CD45RA ⁺ CCR7 ^{mid} CD27 ⁺ CD127 ⁻ CD29 ⁻ Tbet ⁻
16	CD45RA ⁺ CCR7 ⁻ CD27 ⁺ CD127 ⁺ CD29 ^{hi} Tbet ⁺
17	CD45RA ⁺ CCR7 ⁻ CD27 ⁺ CD127 ⁺ CD29 ⁻ Tbet ⁻
18	CD45RO ⁺ CCR7 ⁻ CD27 ⁻ CD127 ⁻ CD29 ⁺ Tbet ⁺
19	CD45RO ⁺ CCR7 ⁻ CD27 ^{hi} CD127 ⁺ CD29 ⁺ Tbet ⁺ CD49d ^{mid}
20	CD45RA ⁺ CCR7 ⁻ CD27 ⁺ CD127 ⁻ CD29 ^{mid} Tbet ^{hi}
21	Almost all markers low
22	CD45RA ⁺ CCR7 ⁺ CD27 ⁺ CD127 ⁺ CD29 ⁻ Tbet ⁻

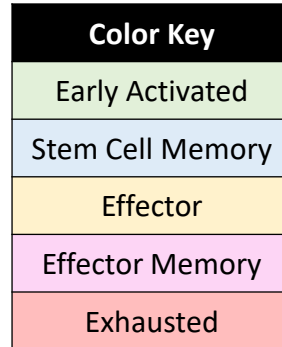


Figure S4

Spider plot depicting longitudinal patient-specific H3.3K27M-reactive CD8+ T-cell frequencies of both Strata A+B patients and Stratum A patients alone

Table S1

Table depicting multivariate cox proportional hazards analyses using overall survival for both Strata A+B and Stratum A patients alone for non-confounding immune profiles

Strata A+B Patients

Table S1: Multivariate Analysis of Immune Profiles

Parameter	Condition	Hazard Ratio* (95% CI)	P-value	Confounding (P-value via Fisher's Exact Test)			
				Immunological Response	Bulk CD8+ T-cell Expansion	Baseline MDSC Abundance	H3.3K27M-reactive T _{EX} Expansion
Immunological Response	No (n=11)	Reference					
	Yes (n=7)	0.04 (0.004 – 0.045)	p < 0.01**		p = 0.33	p = 0.34	p = 0.32
Bulk CD8+ T-cell Expansion	No (n=13)	Reference					
	Yes (n=5)	4.00 (0.67 – 23.88)	p = 0.13			p = 1.00	p = 0.61
Baseline MDSC Abundance	High (n=14)	Reference					
	Low (n=14)	0.34 (0.08 – 1.51)	p = 0.15				p = 0.62
H3.3K27M-reactive T_{EX} Expansion	No (n=6)	Reference					
	Yes (n=12)	3.75 (0.85 – 16.54)	p = 0.08				

Stratum A Patients

Parameter	Condition	Hazard Ratio (95% CI)	P-value	Confounding (P-value via Fisher's Exact Test)			
				Immunological Response	Bulk CD8+ T-cell Expansion	Baseline MDSC Abundance	H3.3K27M-reactive T _{EX} Expansion
Immunological Response	No (n=6)	Reference					
	Yes (n=6)	0.03 (0.001 – 1.960)	p = 0.10		p = 0.55	p = 1.00	p = 0.55
Bulk CD8+ T-cell Expansion	No (n=8)	Reference					
	Yes (n=4)	15.21 (0.33 – 668.70)	p = 0.16			p = 0.58	p = 1.00
Baseline MDSC Abundance	High (n=10)	Reference					
	Low (n=9)	0.09 (0.01 – 0.92)	p = 0.04*				p = 0.58
H3.3K27M-reactive T_{EX} Expansion	No (n=4)	Reference					
	Yes (n=8)	2.12 (0.30 – 14.92)	p = 0.45				

*Hazard ratios derived from overall survival

Figure S5

Kaplan-Meier survival curves visualizing OS among strata A + B patients based on the expansion of H3.3K27M-reactive CD8+ T-cell subpopulations.

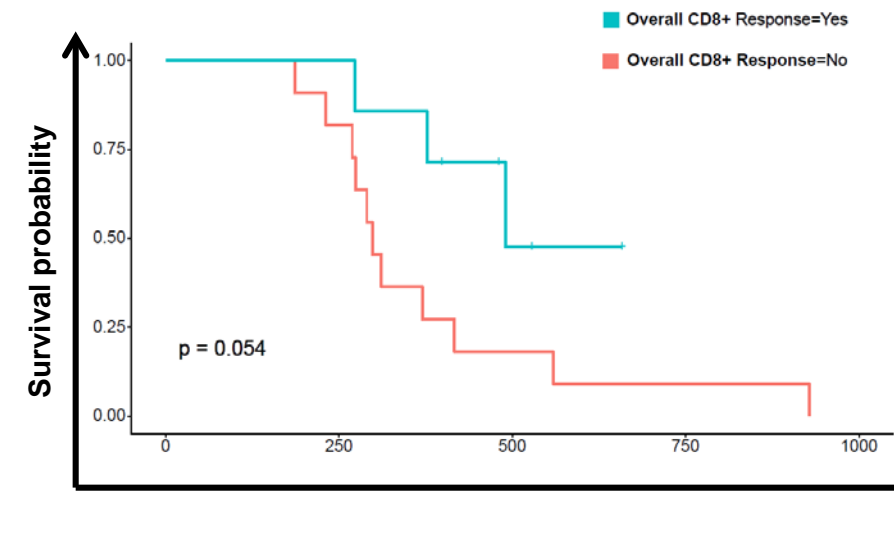
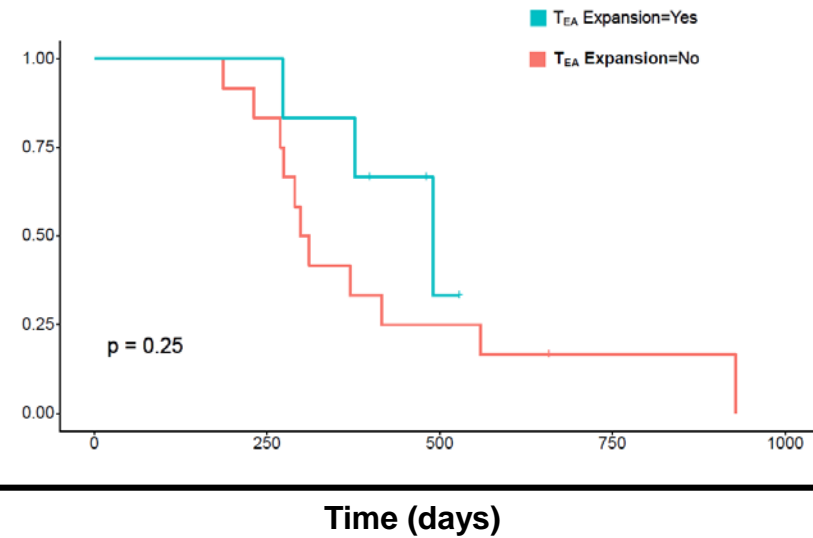
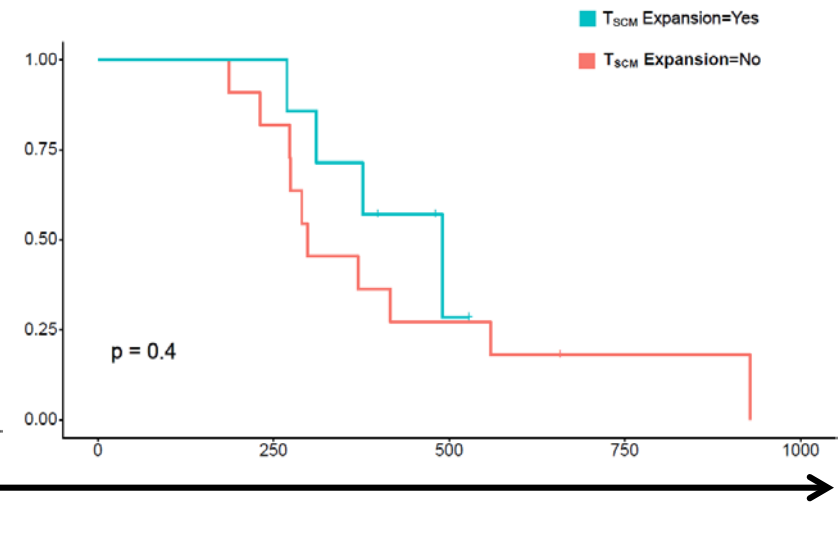
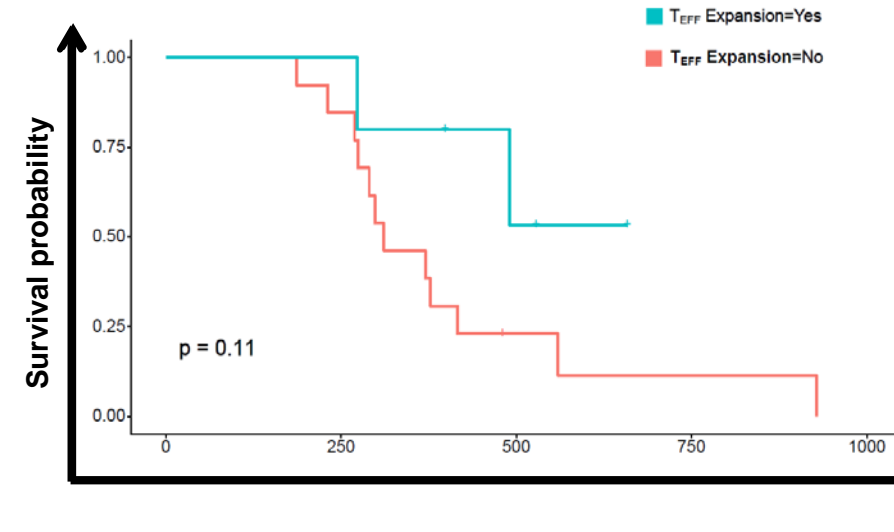
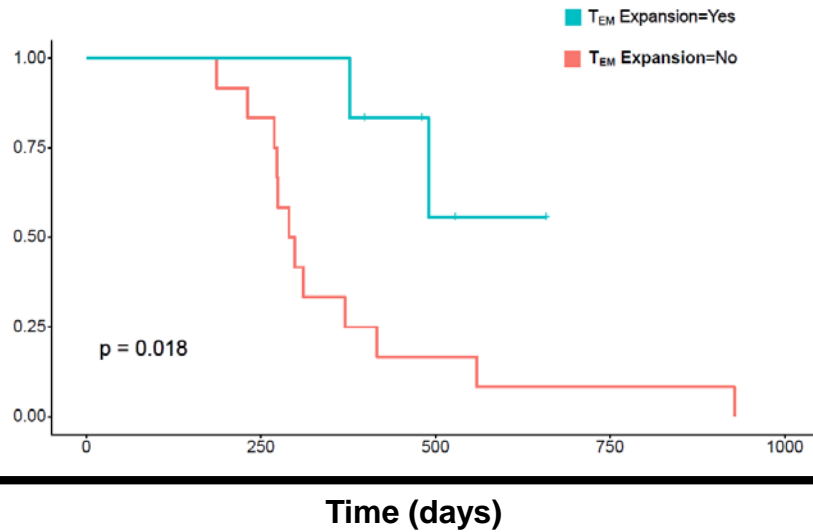
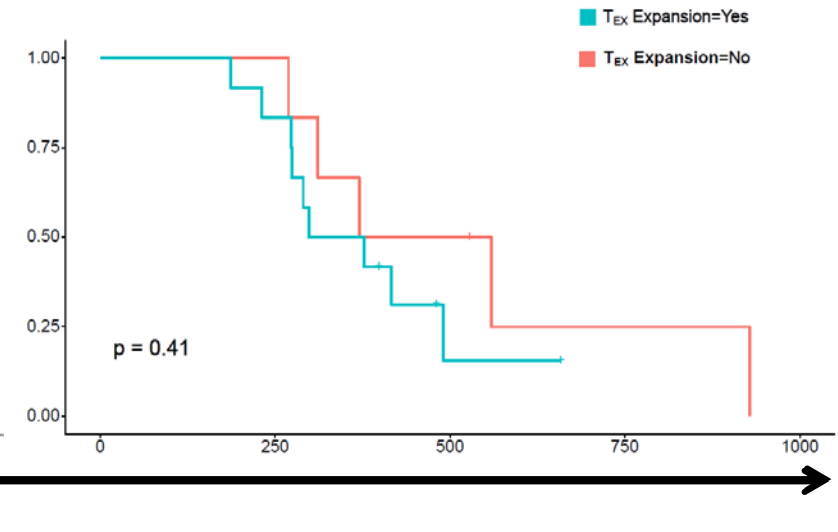
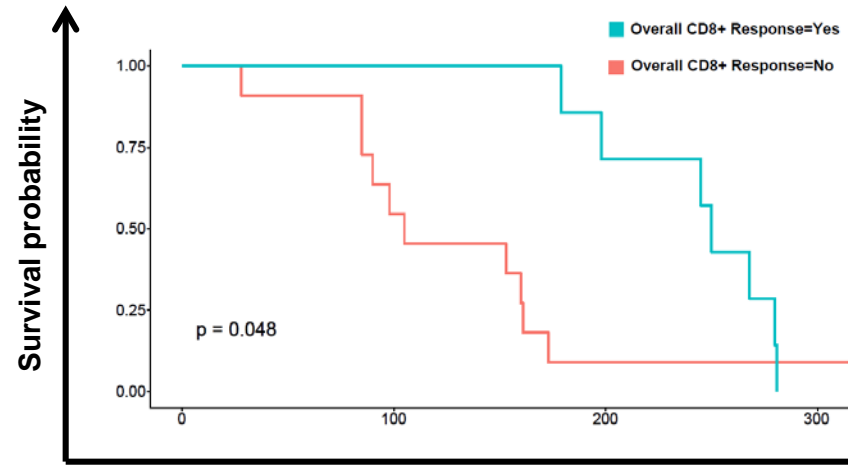
Overall CD8+**Early Activated CD8+****Stem Cell Memory CD8+****Effector CD8+****Effector Memory CD8+****Exhausted CD8+**

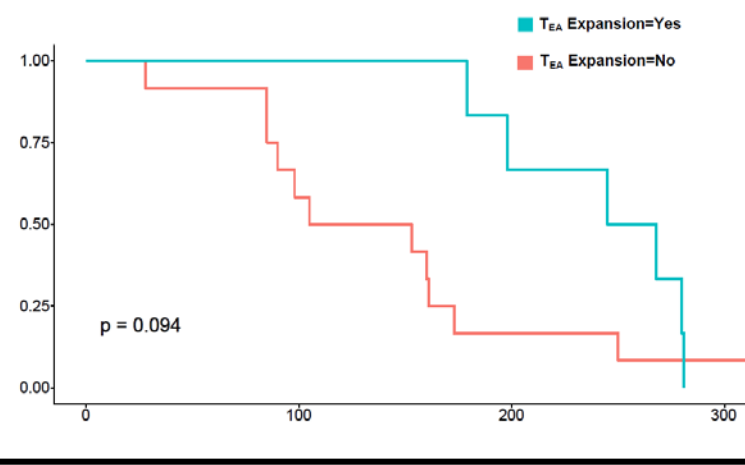
Figure S6

Kaplan-Meier survival curves visualizing PFS among strata A + B patients based on the expansion of H3.3K27M-reactive CD8+ T-cell subpopulations.

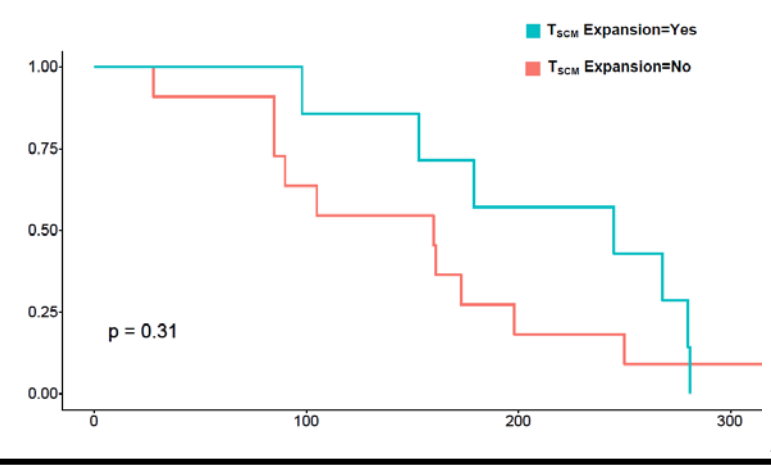
Overall CD8+



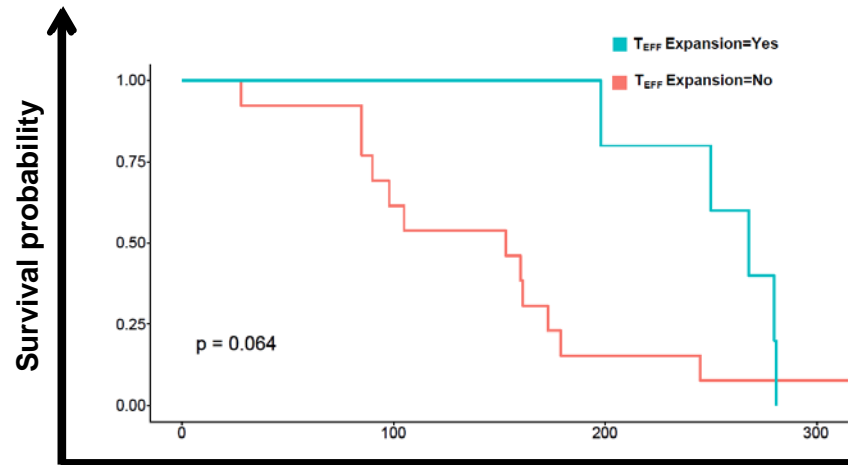
Early Activated CD8+



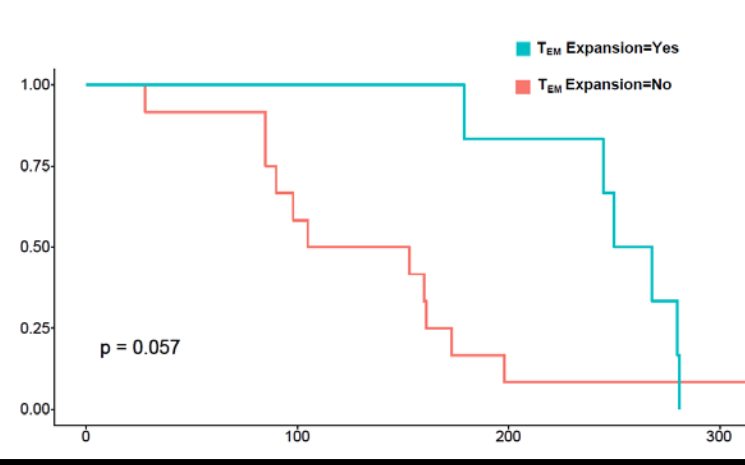
Stem Cell Memory CD8+



Effector CD8+



Effector Memory CD8+



Exhausted CD8+

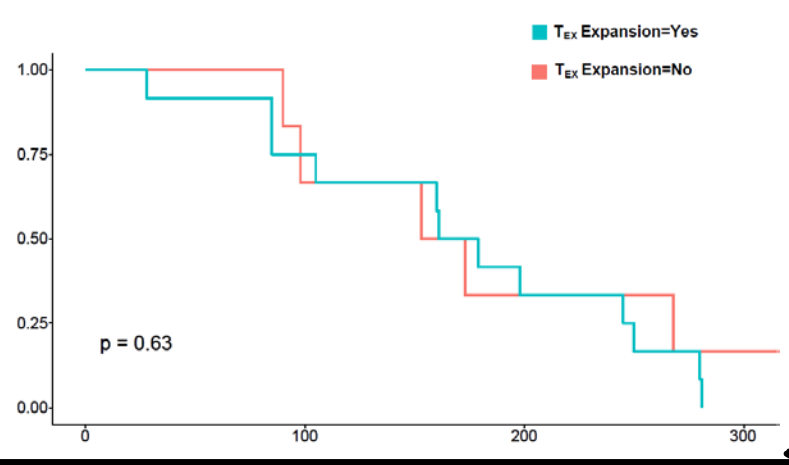


Figure S7

Kaplan-Meier survival curves visualizing OS among stratum A patients based on the expansion of H3.3K27M-reactive CD8+ T-cell subpopulations.

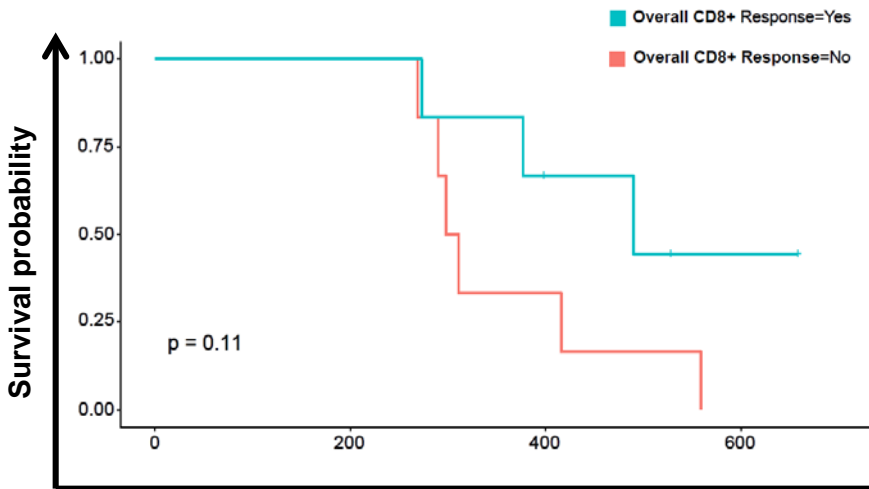
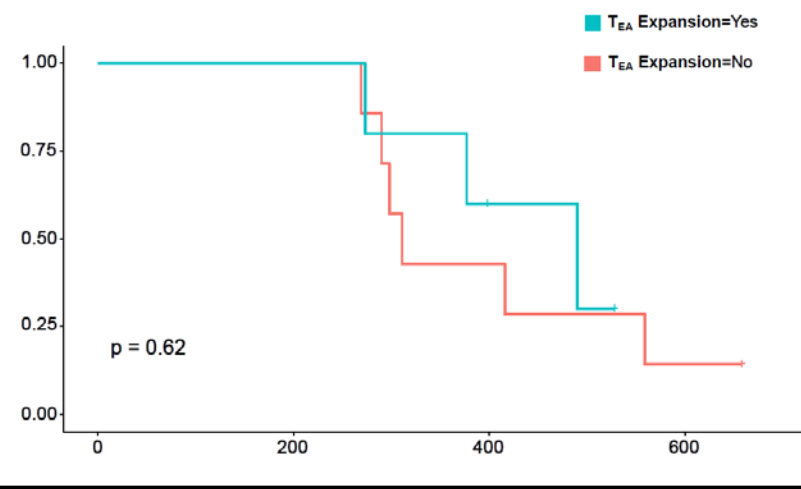
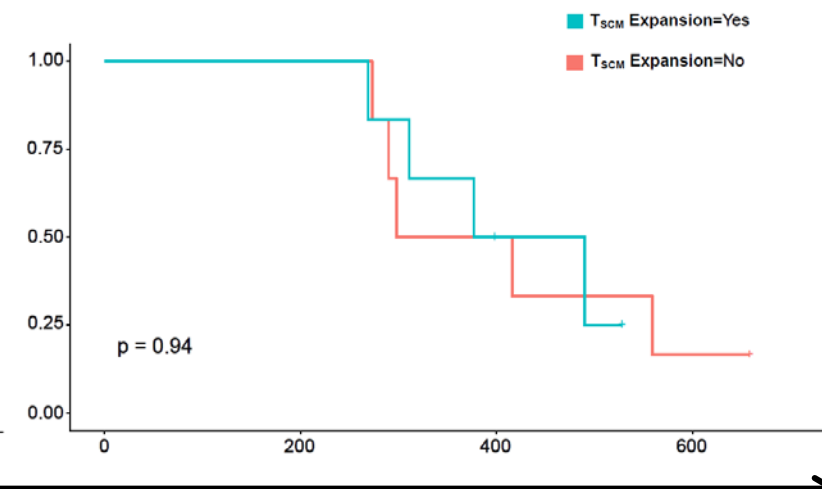
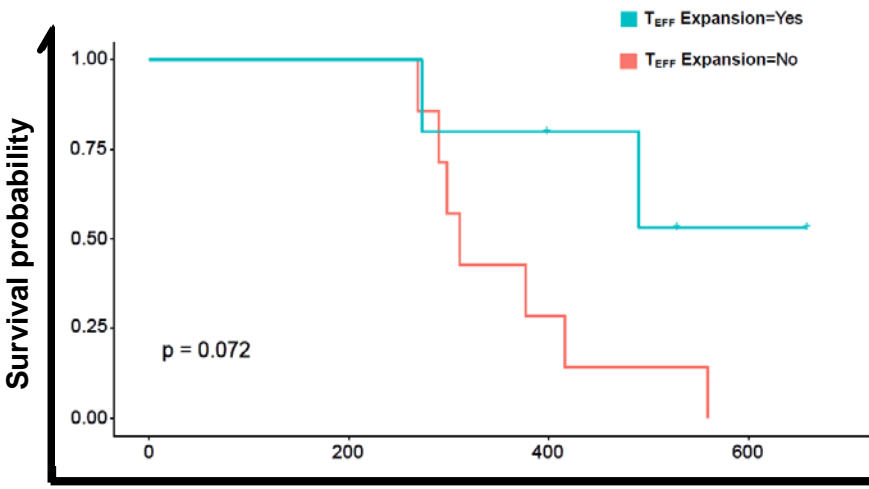
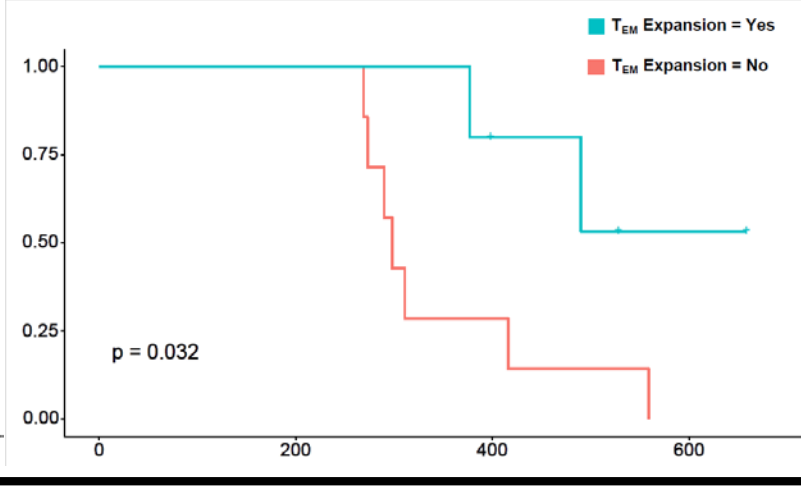
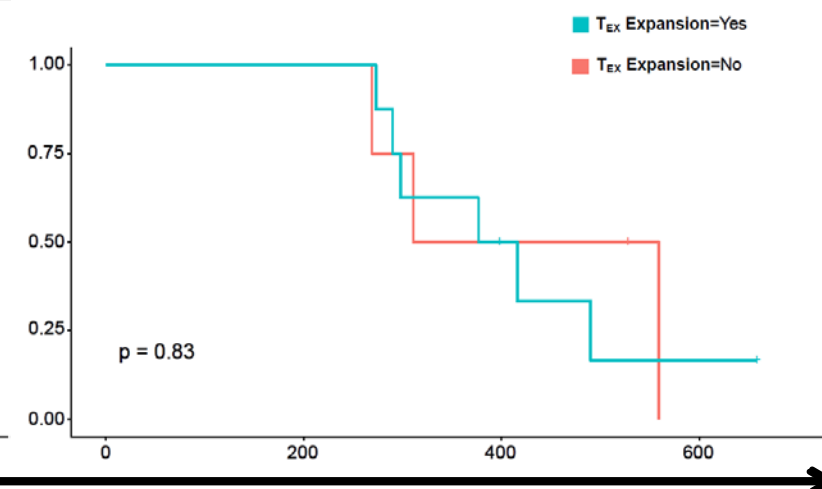
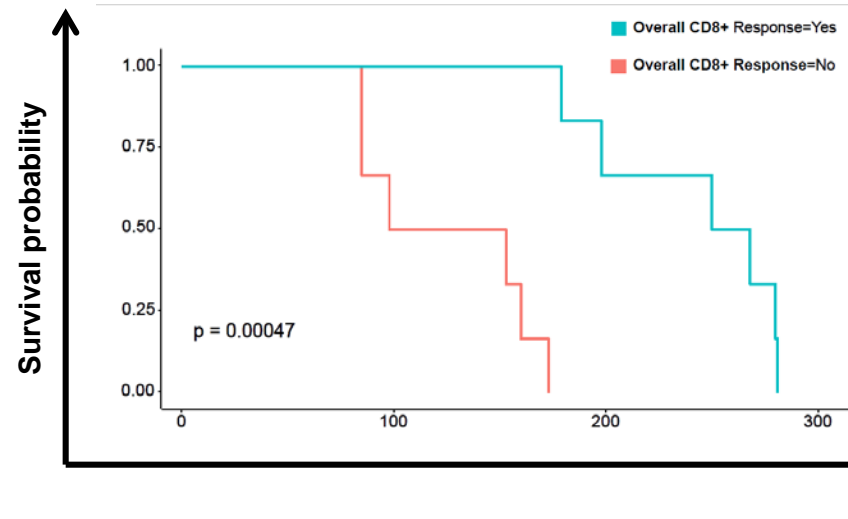
Overall CD8+**Early Activated CD8+****Stem Cell Memory CD8+****Effector CD8+****Effector Memory CD8+****Exhausted CD8+**

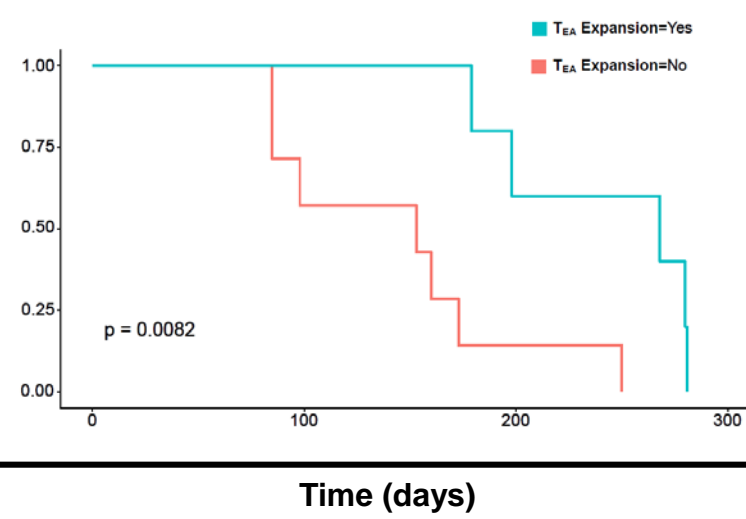
Figure S8

Kaplan-Meier survival curves visualizing PFS among stratum A patients based on the expansion of H3.3K27M-reactive CD8+ T-cell subpopulations.

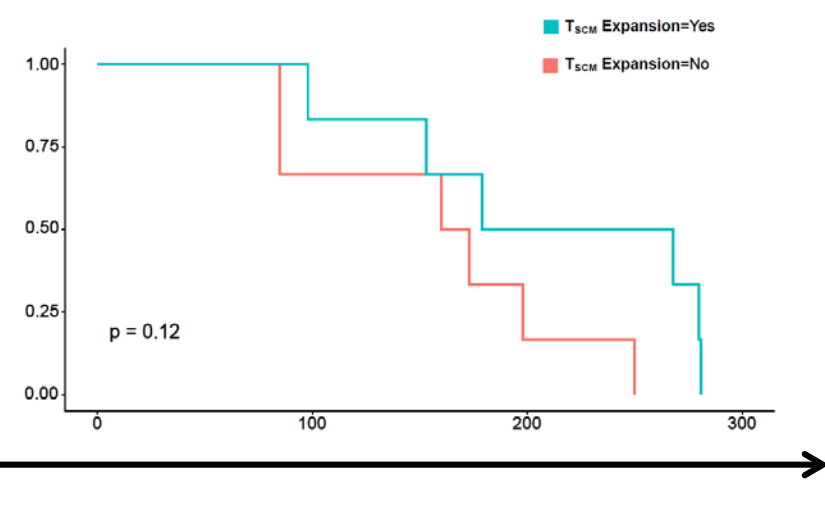
Overall CD8+



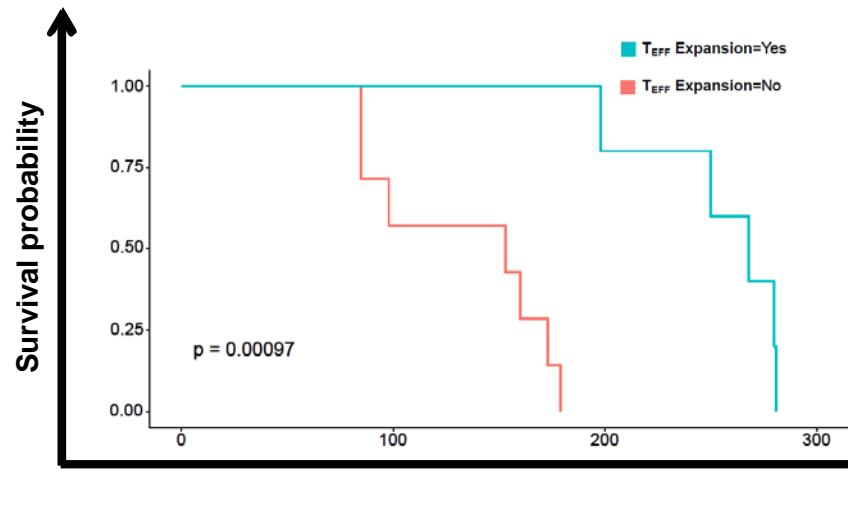
Early Activated CD8+



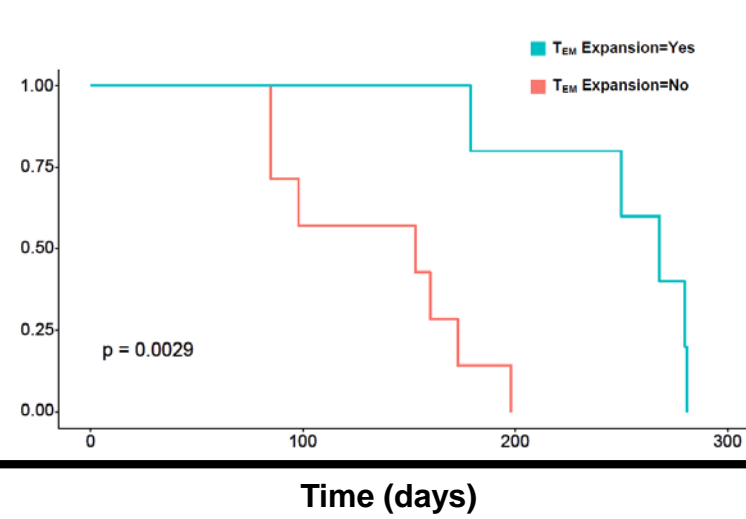
Stem Cell Memory CD8+



Effector CD8+



Effector Memory CD8+



Exhausted CD8+

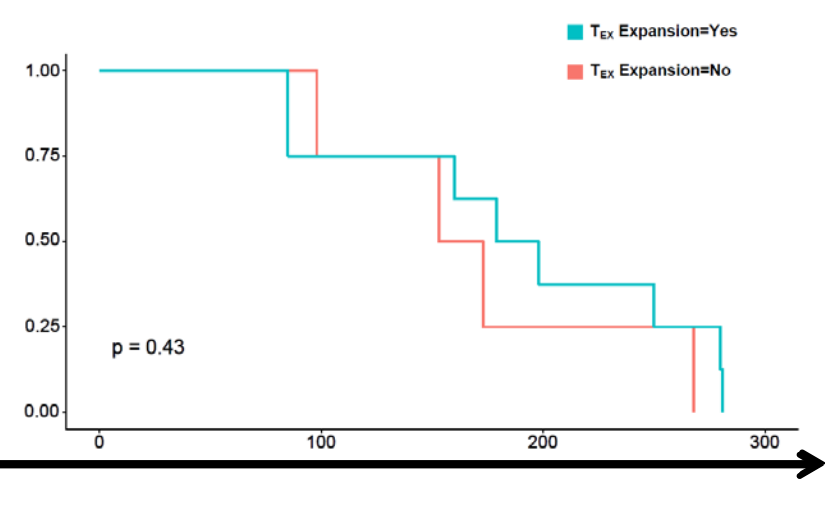
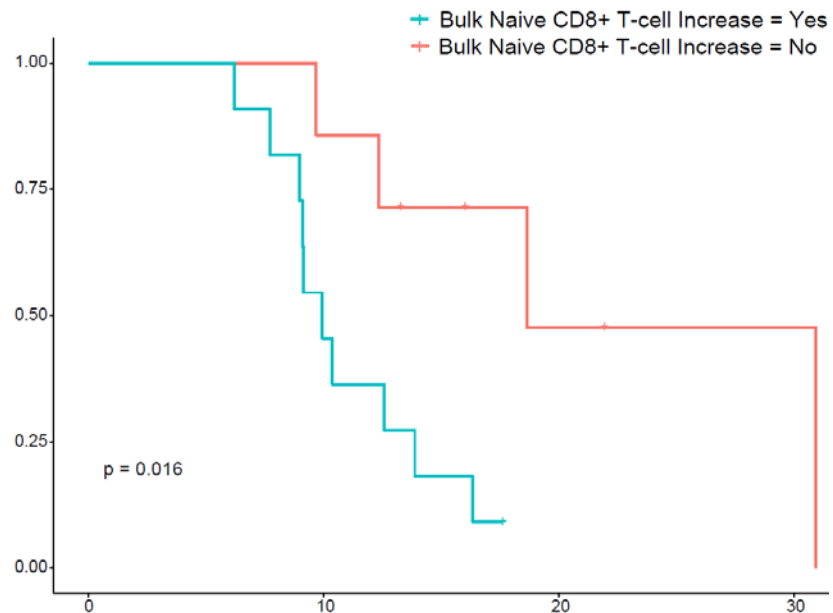


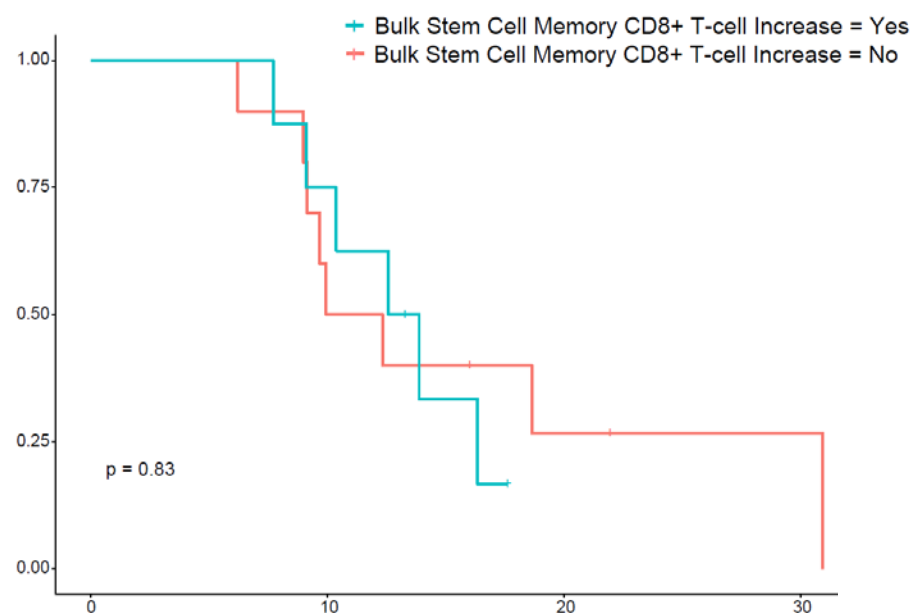
Figure S9

Kaplan-Meier survival curves visualizing OS among strata A + B patients based on the expansion of bulk CD8+ T-cell subpopulations.

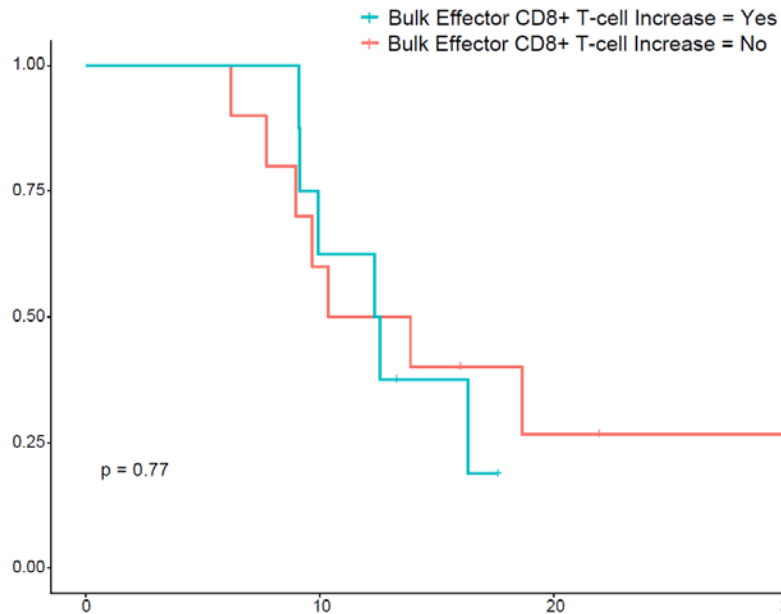
Early Activated CD8+



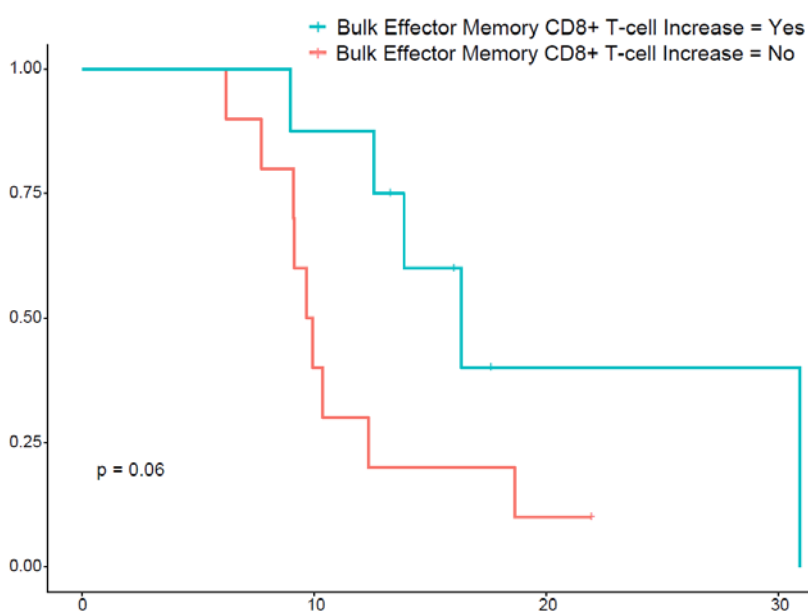
Stem Cell Memory CD8+



Effector CD8+



Effector Memory CD8+



Exhausted CD8+

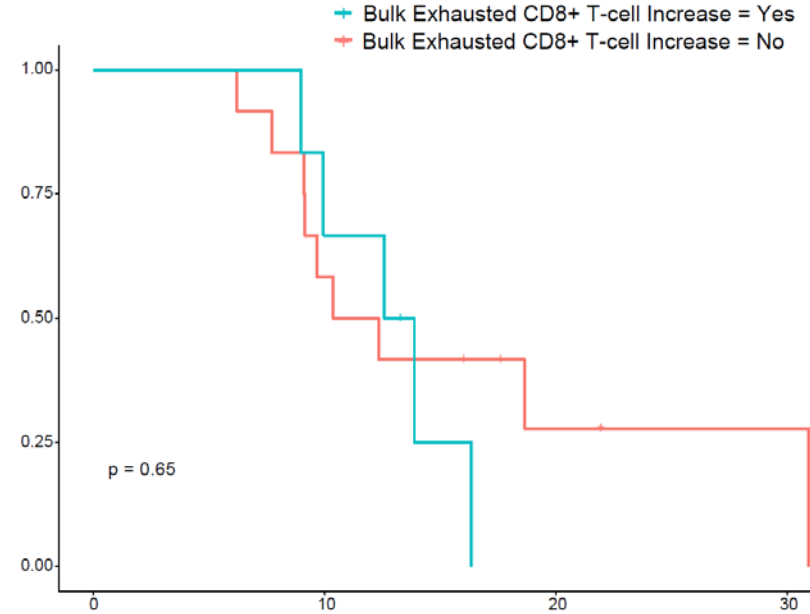
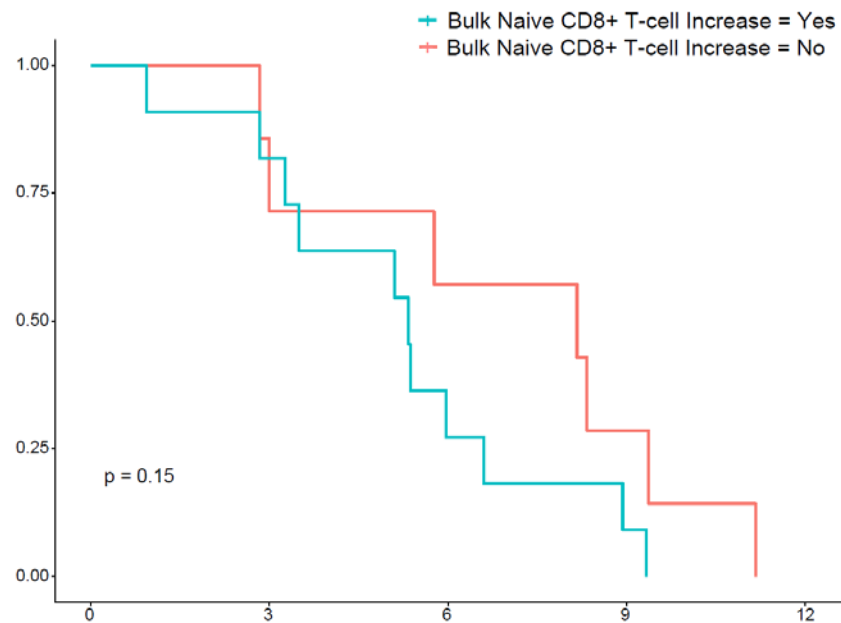


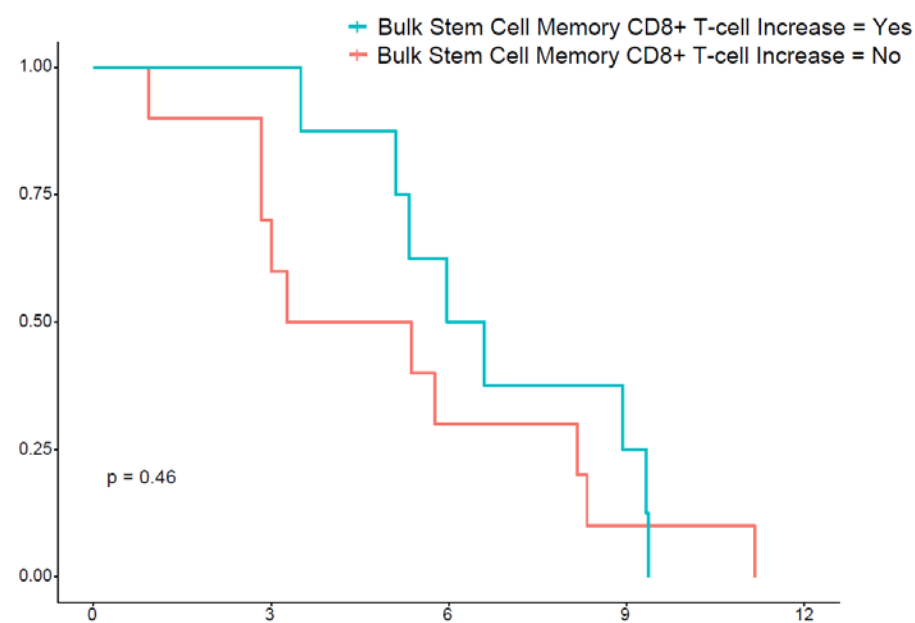
Figure S10

Kaplan-Meier survival curves visualizing PFS among strata A + B patients based on the expansion of bulk CD8+ T-cell subpopulations.

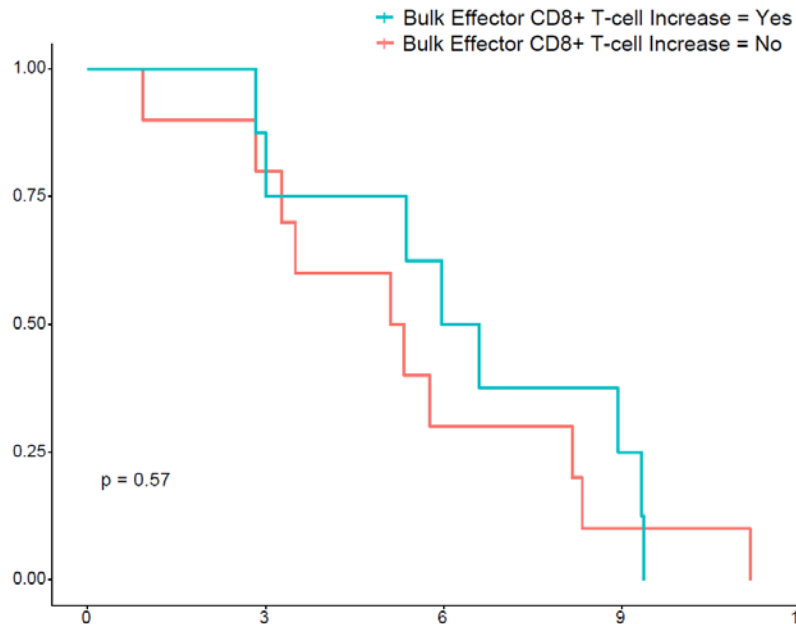
Early Activated CD8+



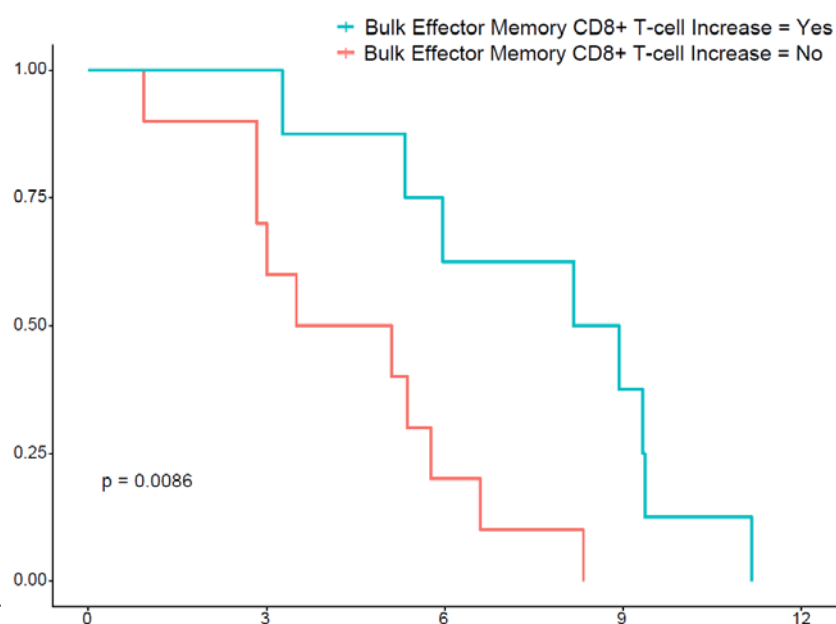
Stem Cell Memory CD8+



Effector CD8+



Effector Memory CD8+



Exhausted CD8+

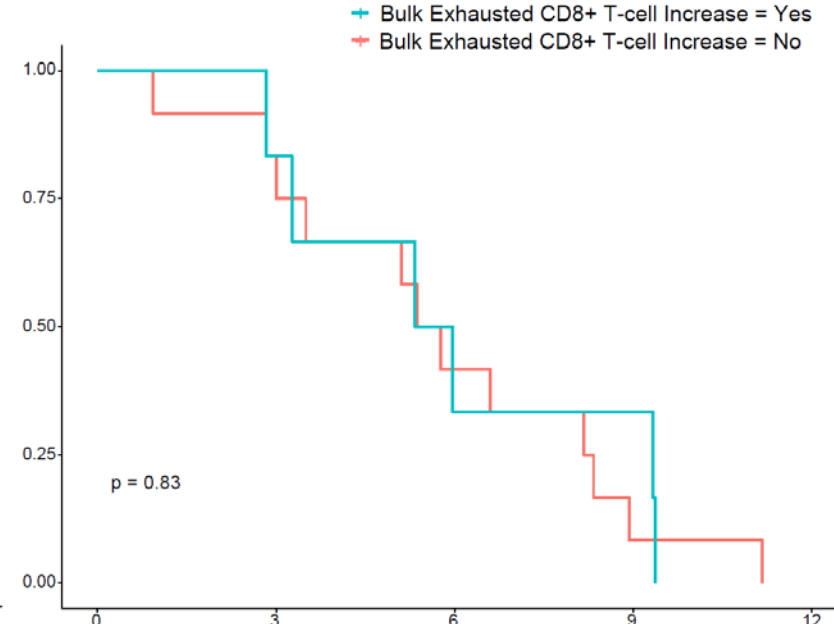
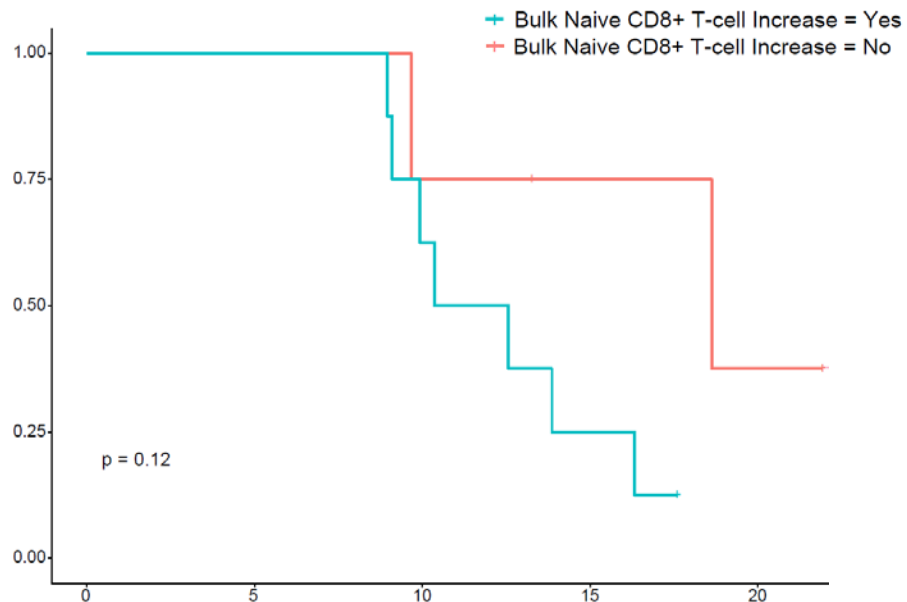


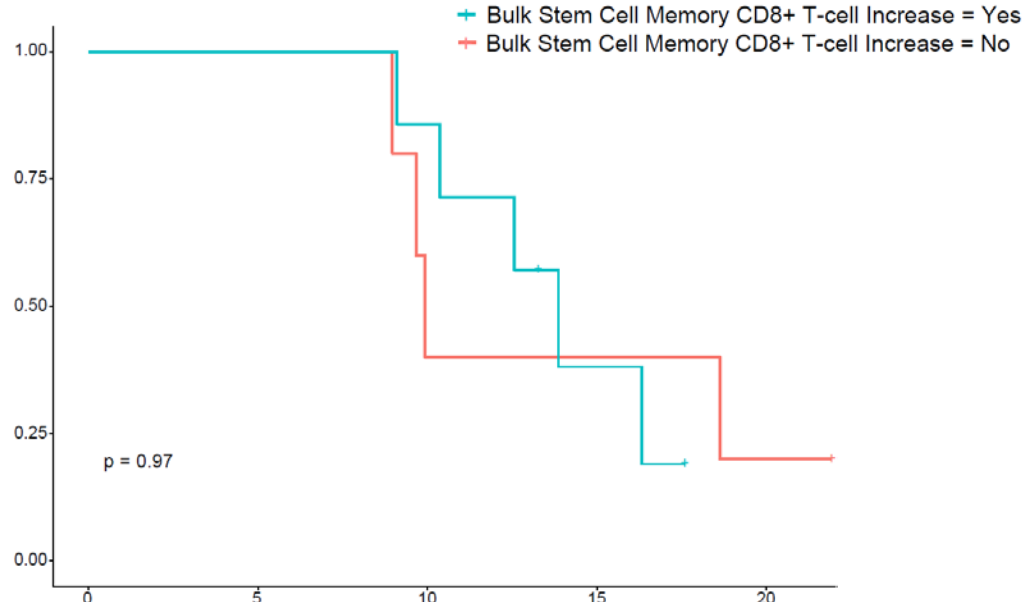
Figure S11

Kaplan-Meier survival curves visualizing OS among stratum A patients based on the expansion of bulk CD8+ T-cell subpopulations.

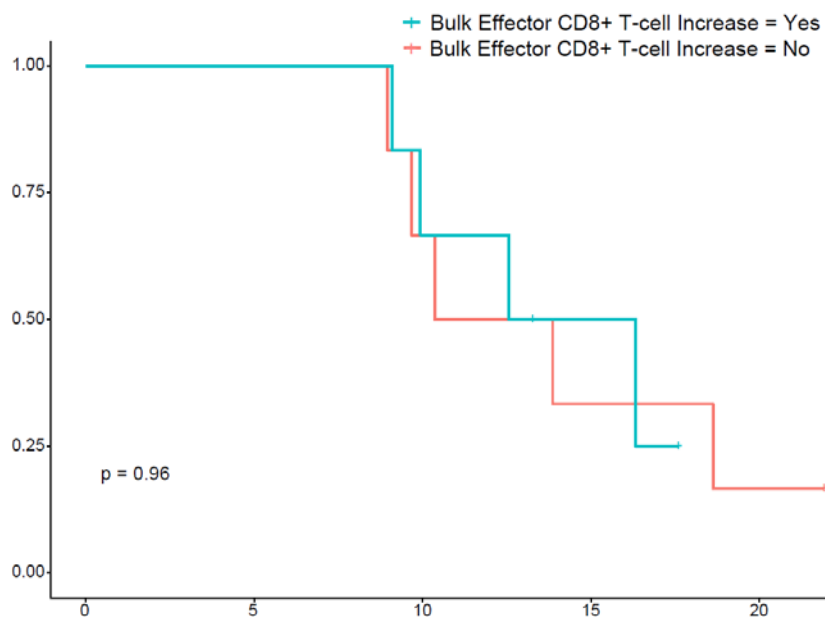
Early Activated CD8+



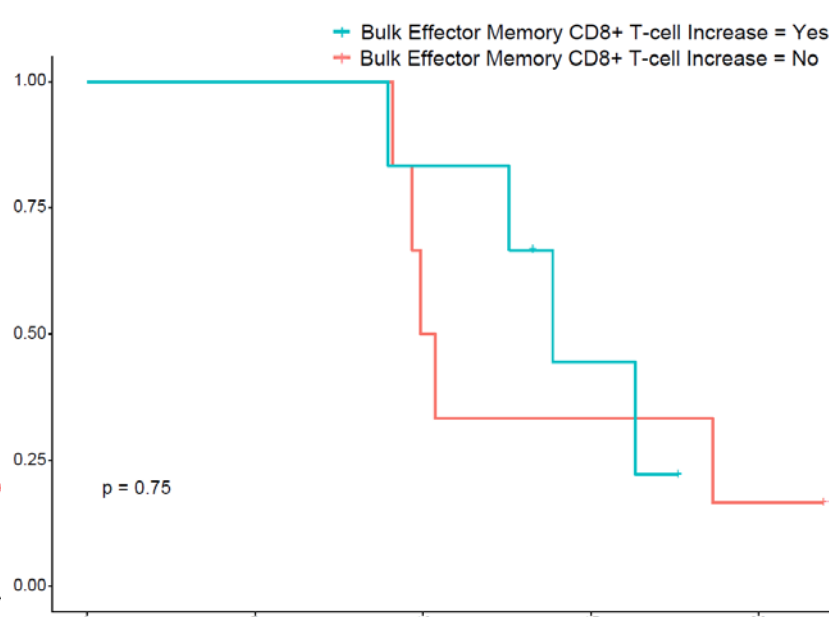
Stem Cell Memory CD8+



Effector CD8+



Effector Memory CD8+



Exhausted CD8+

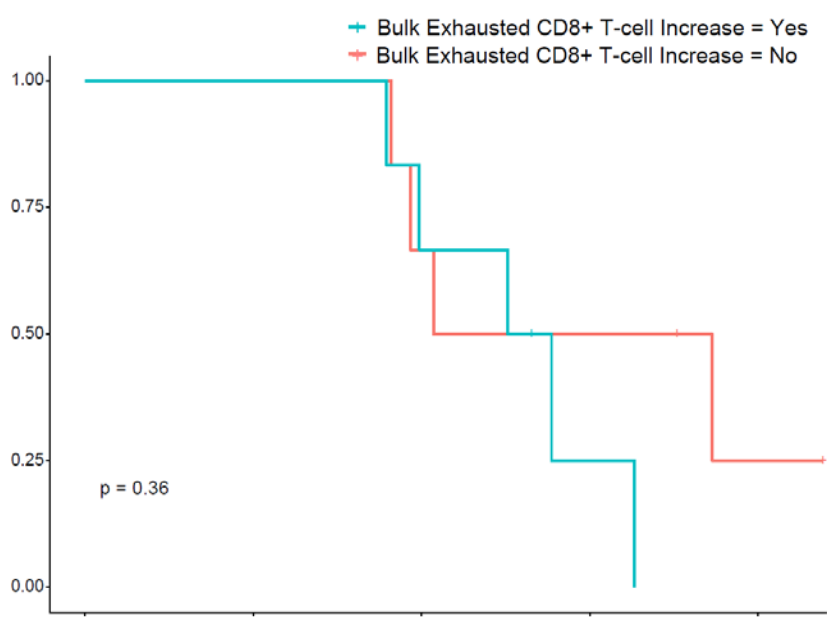
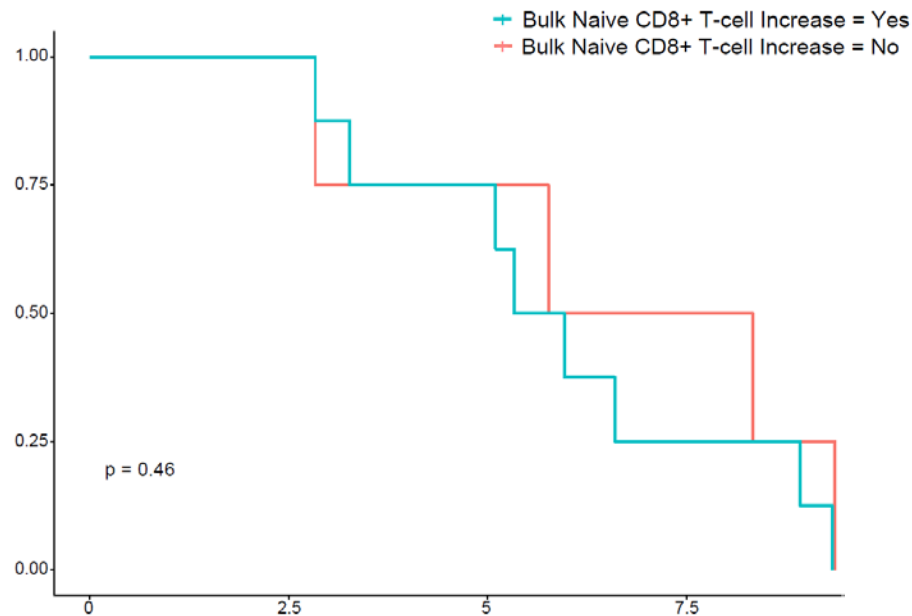


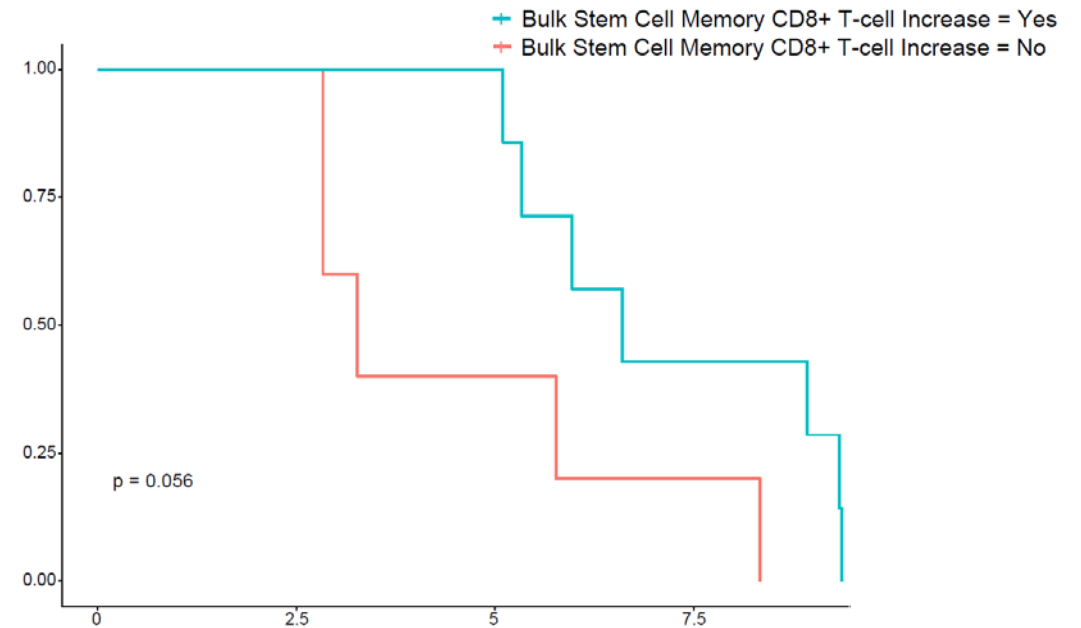
Figure S12

Kaplan-Meier survival curves visualizing PFS among stratum A patients based on the expansion of bulk CD8+ T-cell subpopulations.

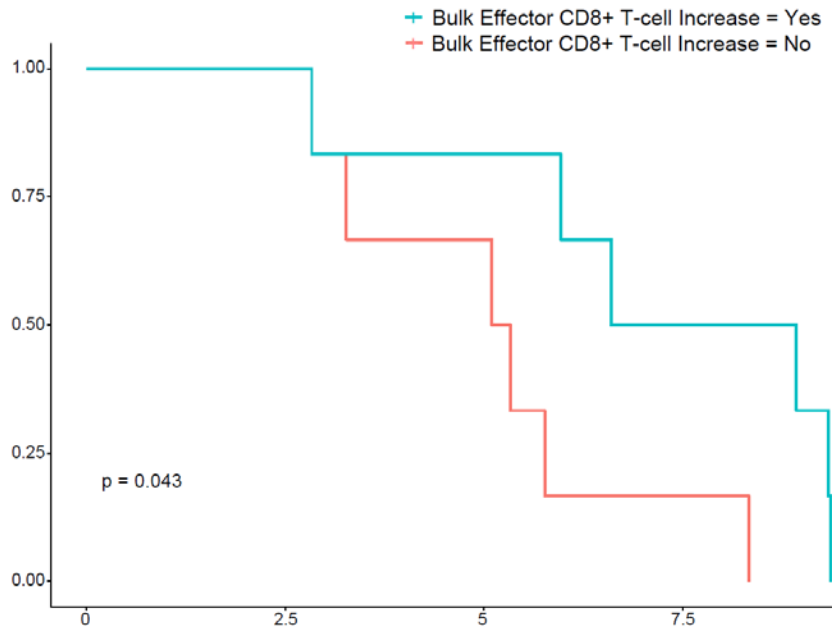
Early Activated CD8+



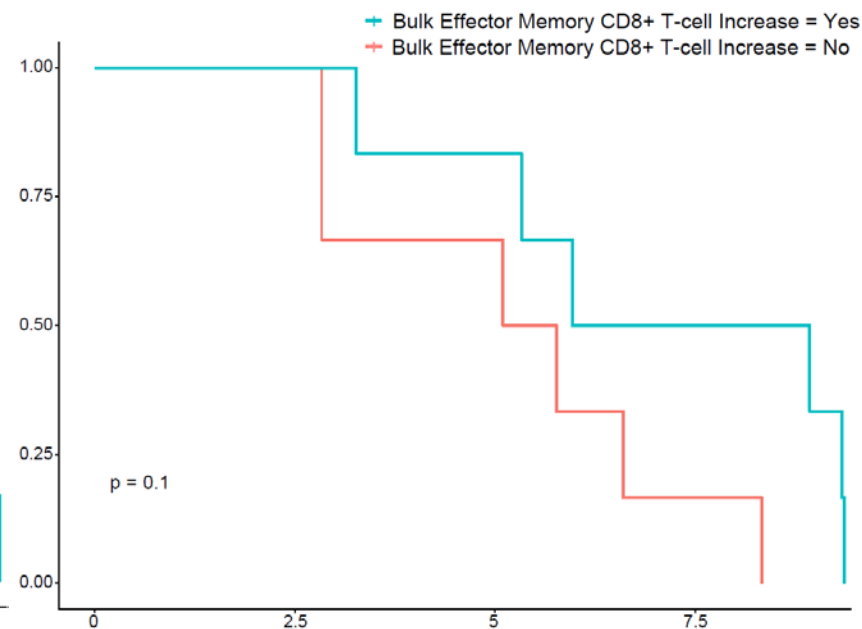
Stem Cell Memory CD8+



Effector CD8+



Effector Memory CD8+



Exhausted CD8+

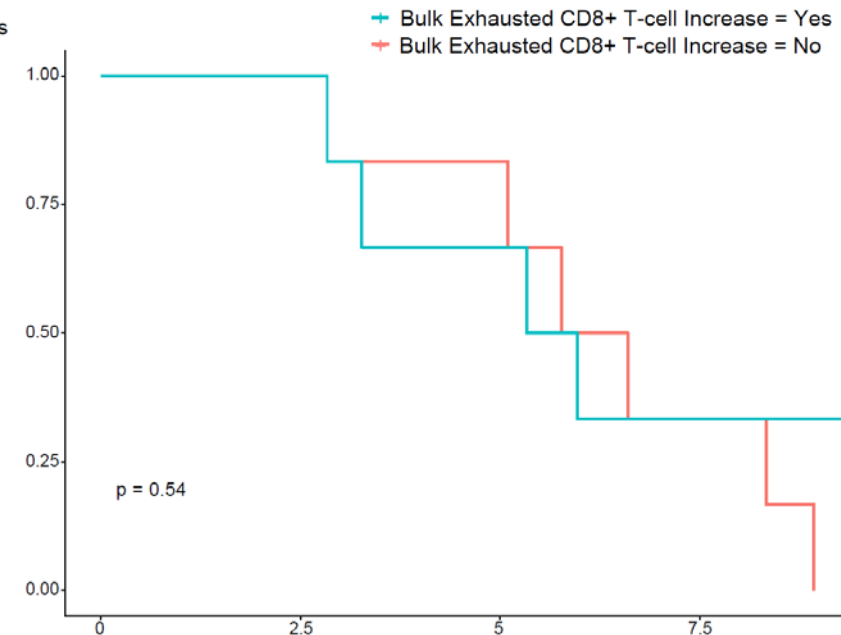


Figure S13

Linear model correlating the relationship between number of vaccines administered and relative percent change of H3.3K27M-reactive CD8+ T-cells utilizing Spearman correlation coefficient. Models both with and without outlier patient exhibiting greatest H3.3K27M-reactive CD8+ T-cell expansion (PNOC007-25) reveal significant correlation.

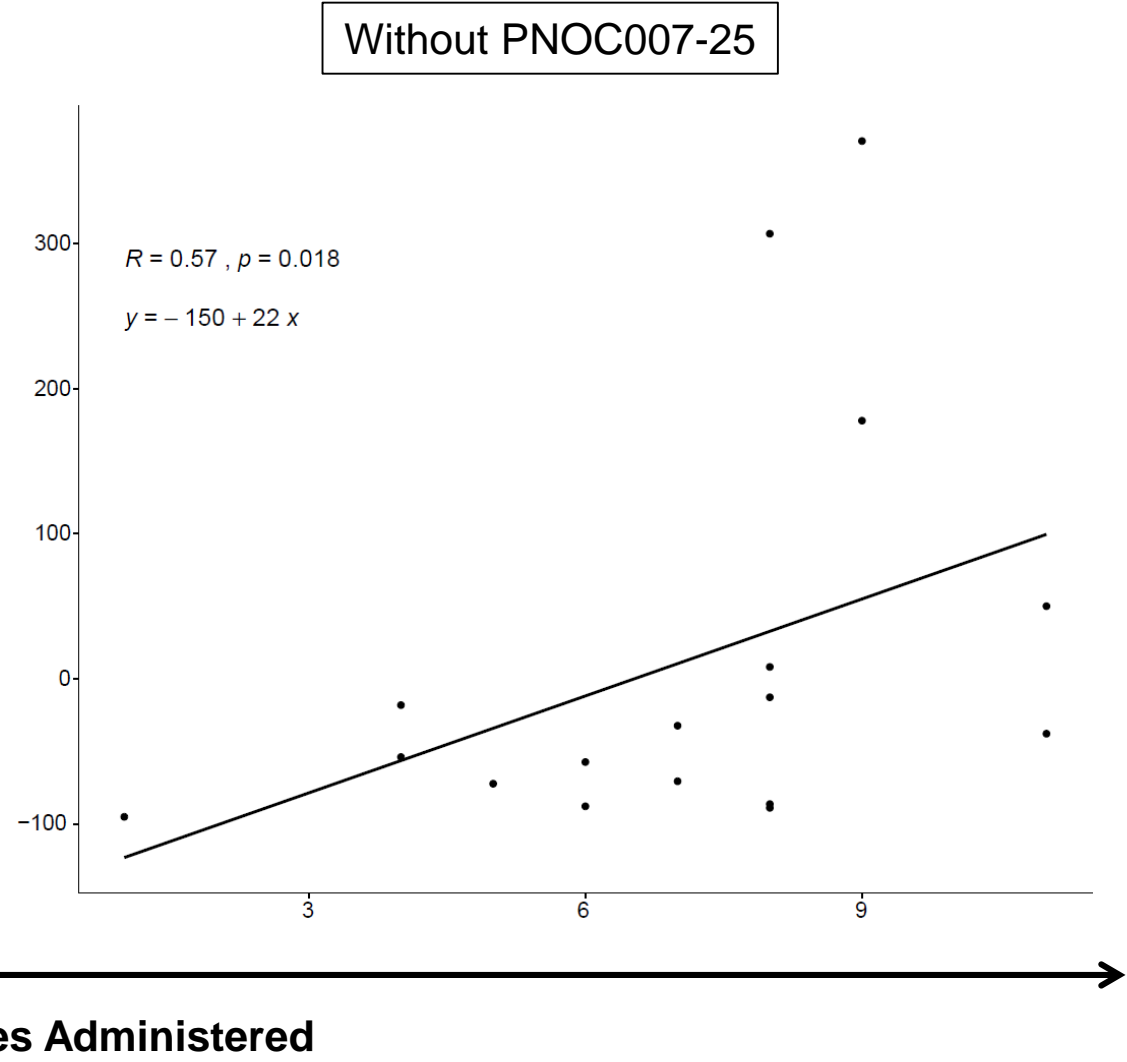
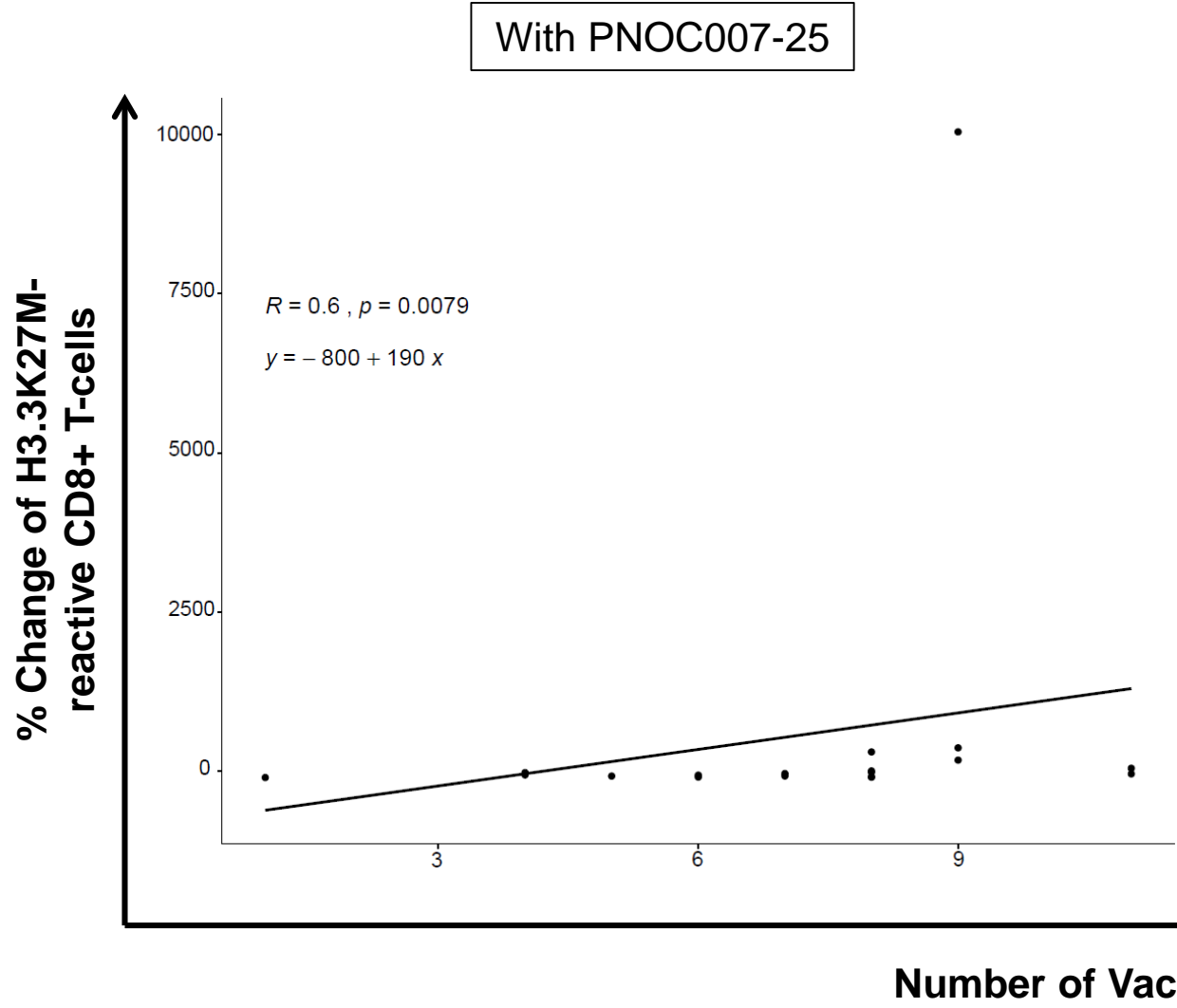


Figure S14

tSNE stratification and expression profiles of discrete myeloid subpopulations.

Left, patient-derived myeloid cells were stratified on a tSNE plot using the myeloid canonical markers: CD33, CD11b, CD11c, CD14, CD15 and CD16. *Right*, heat map visualizing the z-score normalized expression of resultant myeloid cell clusters.

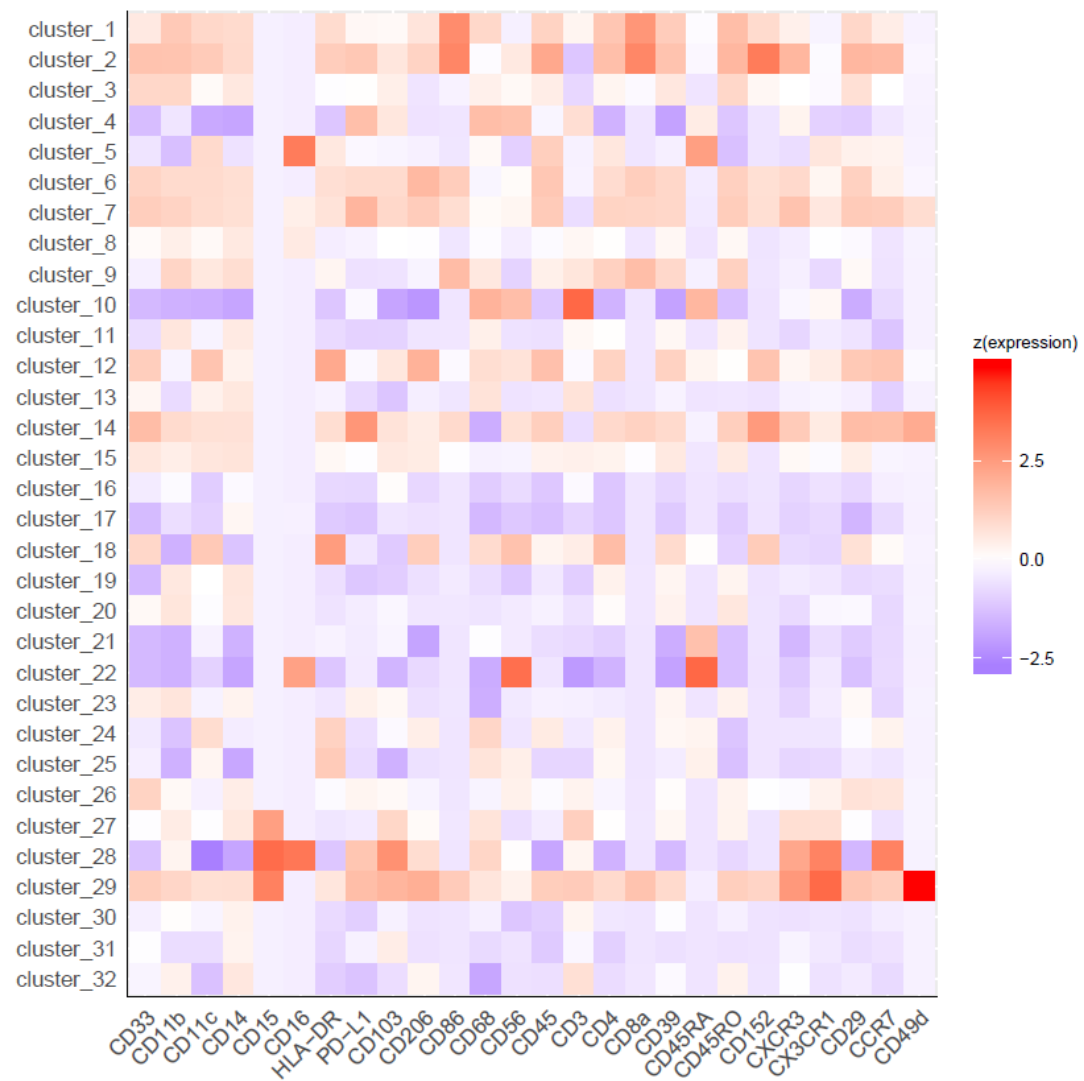
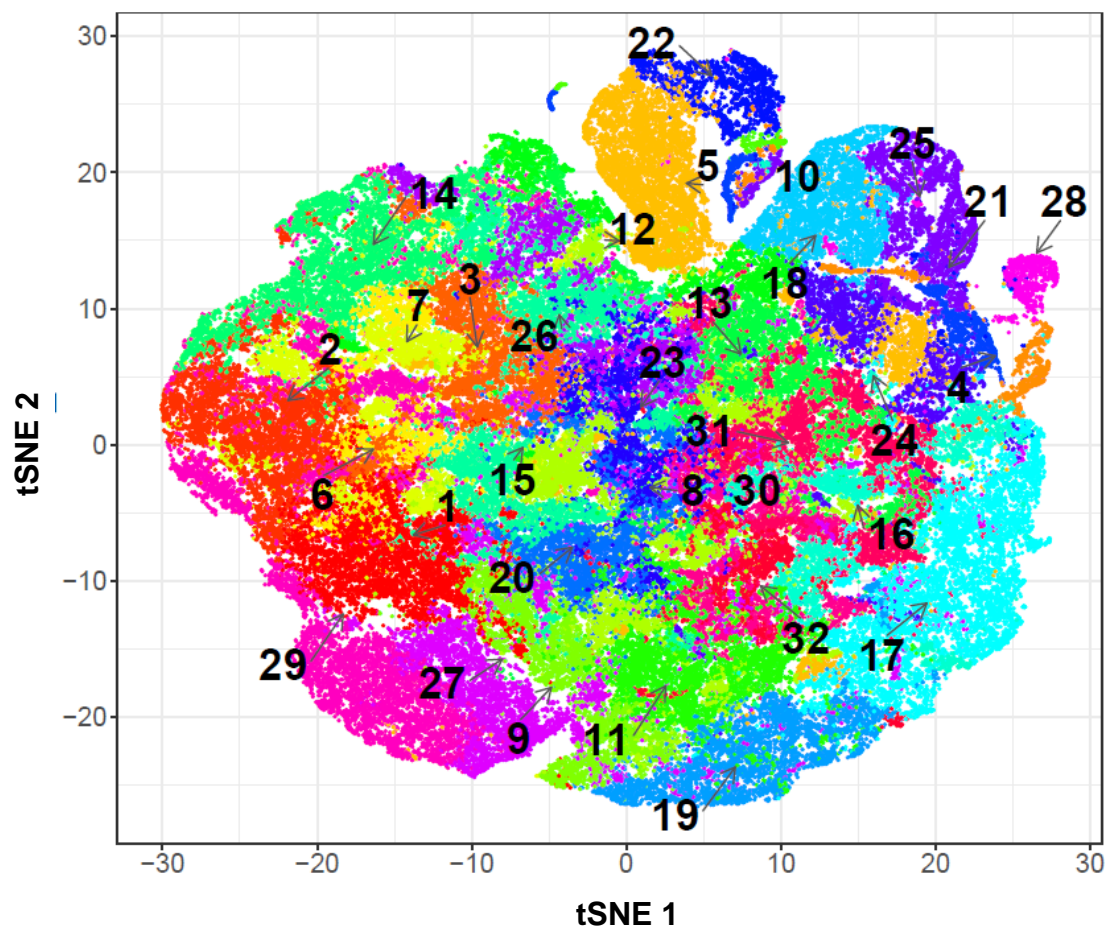


Table S2

CytoTOF-based marker expression profiles and MDSC phenotypic characterizations of myeloid cell clusters identified via tSNE stratification.

Cluster Number	Phenotype
1	CD33+ CD11b+ CD14+ CD86+ CD68 ^{hi}
2	CD33+ CD11b+ CD14+ CD86+ CD68 ^{mid}
3	CD33+ CD11b+ CD11c ^{mid} CD14+ CD206 ^{lo} CD68 ^{mid}
4	Almost all markers low
5	CD11c+ CD16+ HLA-DR+
6	CD33+ CD11b+ CD11c+ CD14+ CD206+ HLA-DR ^{hi}
7	CD33+ CD11b+ CD11c+ CD14+ CD16 ^{hi} HLA-DR ^{hi}
8	CD33 ^{mid} CD11b+ CD11c+ CD14 ^{hi} CD16 ^{hi} HLA-DR ^{lo}
9	CD33 ^{mid} CD11b+ CD11c+ CD14+ HLA-DR ^{mid} CD206-
10	Almost all markers low
11	CD33 ^{lo} CD11b+ CD11c ^{mid} CD14 ^{hi} CD206- CD68+
12	CD33+ CD11c+ HLA-DR+ CD103 ^{hi} CD206+
13	CD33 ^{hi} CD11b ^{lo} CD11c ^{hi} CD14+ HLA-DR ^{lo} CD68 ^{hi}
14	CD33+ CD11b+ CD11c+ CD14+ HLA-DR ^{hi}
15	CD33+ CD11b+ CD11c+ CD14+ HLA-DR ^{mid-hi} CD103 ^{hi} CD206 ^{hi}
16	CD33 ^{mid} CD11b ^{mid} CD14 ^{lo} HLA-DR ^{lo}
17	CD11b ^{lo} CD14 ^{hi} HLA-DR-
18	CD33+ CD11c+ CD206+ HLA-DR+
19	CD11b+ CD11c ^{mid} CD14+
20	CD33+ CD11b+ CD11c ^{mid} CD14 ^{hi} HLA-DR ^{lo}
21	CD11c ^{mid} HLA-DR ^{mid} CD103 ^{mid} CD68 ^{mid}
22	CD11c ^{lo} CD16+ HLA-DR-
23	CD33+ CD11b+ CD14+ HLA-DR-
24	CD11c+ HLA-DR+ CD206 ^{hi}
25	CD11c+ HLA-DR+ CD68 ^{hi}
26	CD33+ CD11b+ CD14+ HLA-DR ^{mid-lo}
27	CD33+ CD11b+ CD11c ^{mid} CD15+ HLA-DR ^{lo}
28	CD11b+ CD15+ CD16+ HLA-DR ^{lo}
29	CD33+ CD11b+ CD11c ^{hi} CD15+ HLA-DR ^{hi} CD103+
30	CD33 ^{lo} CD11b ^{mid} CD14 ^{hi} HLA-DR ^{lo}
31	CD33 ^{mid} CD11b ^{lo} CD14 ^{hi} HLA-DR ^{lo}
32	CD33 ^{lo} CD11b ^{hi} CD14 ^{hi} HLA-DR ^{lo}

Color Key
E-MDSC
M-MDSC

Figure S15

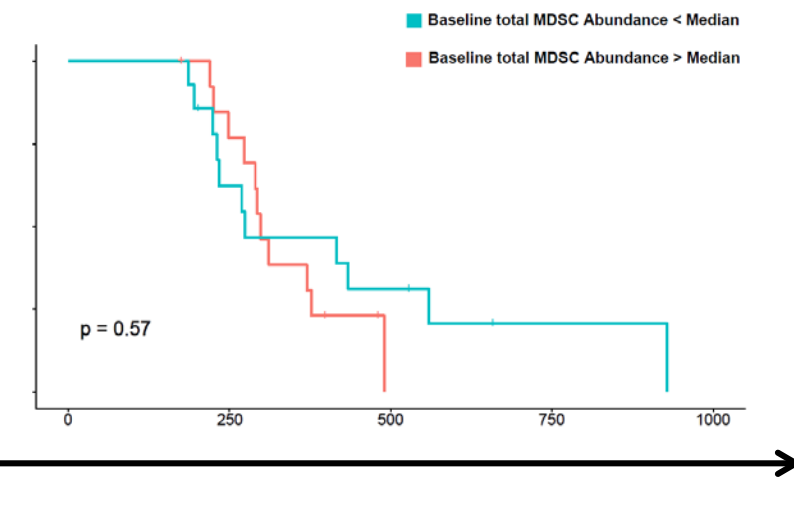
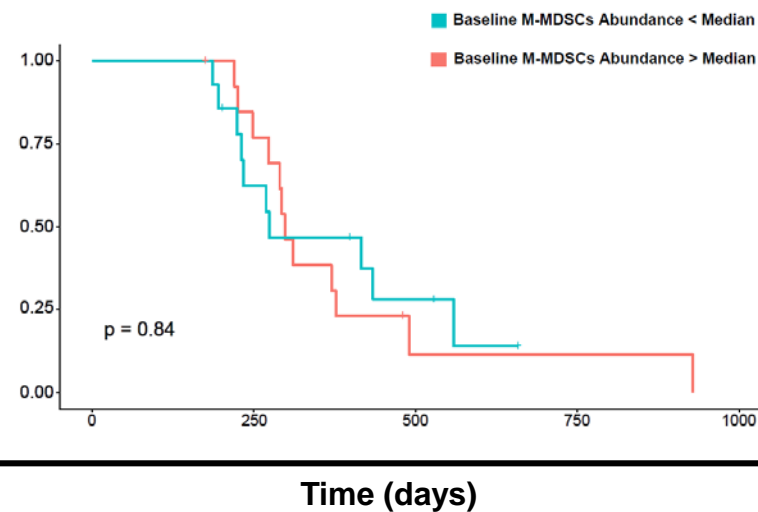
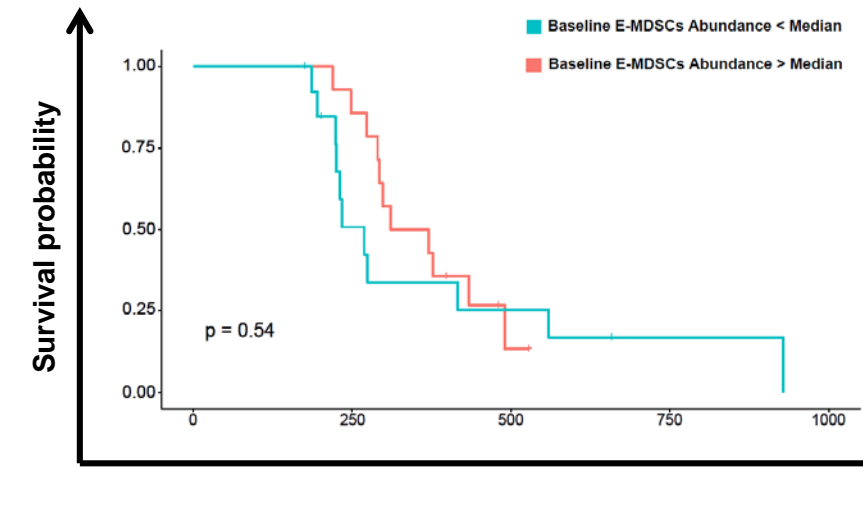
Kaplan-Meier survival curves visualizing OS and PFS among strata A + B patients based on the abundance of circulatory MDSC subtypes at baseline.

OS:

E-MDSCs

M-MDSCs

Total MDSCs



PFS:

E-MDSCs

M-MDSCs

Total MDSCs

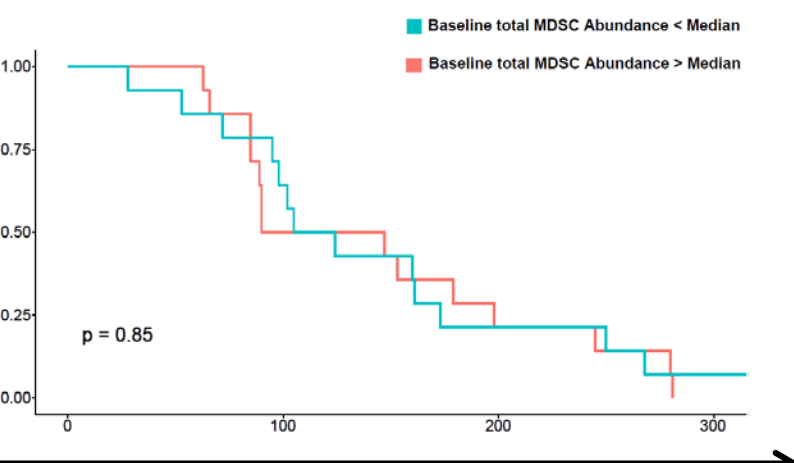
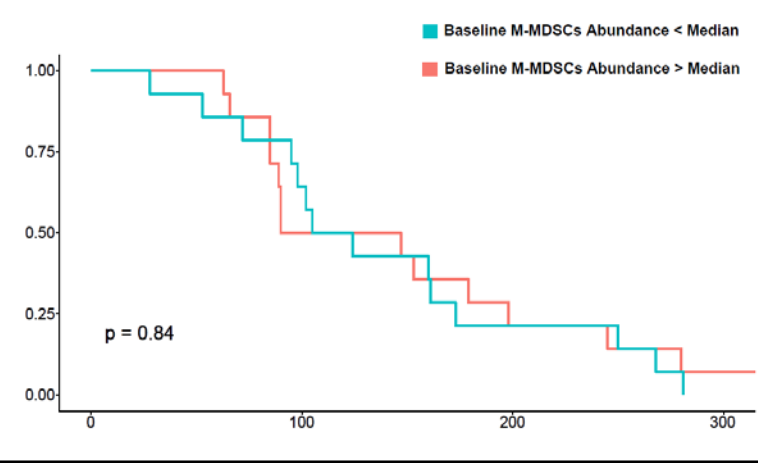
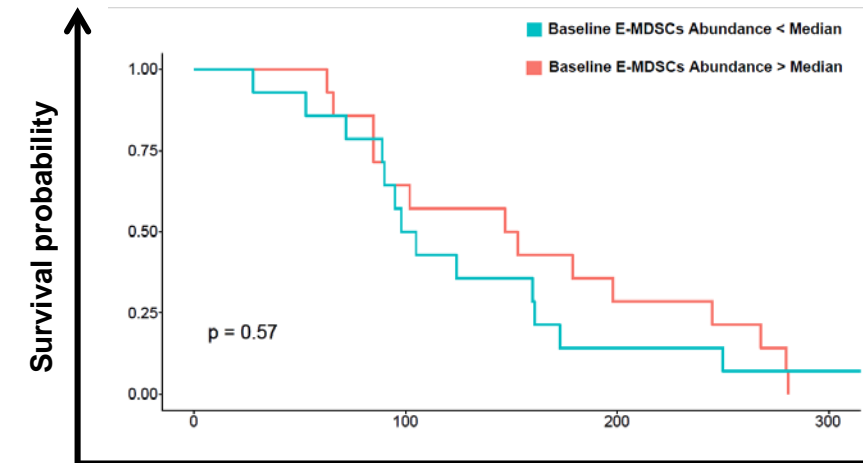


Figure S16

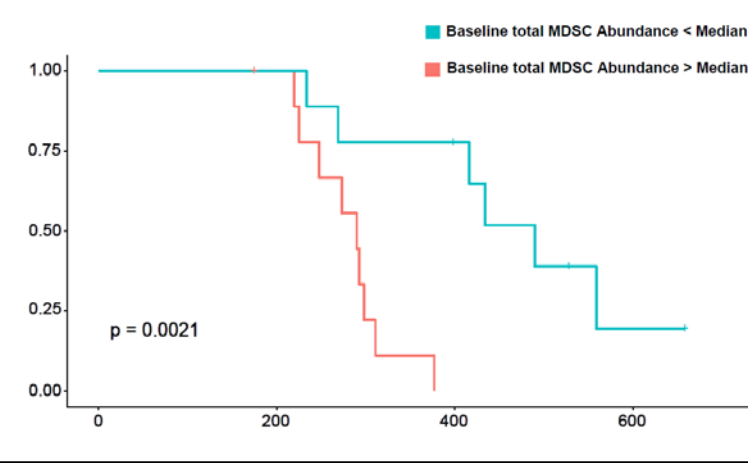
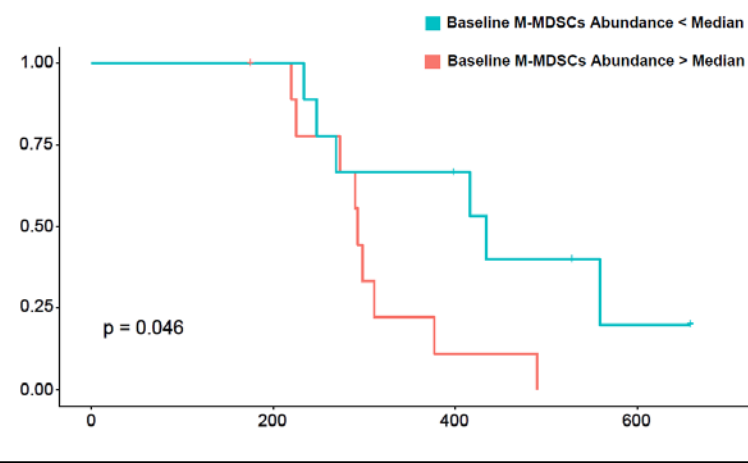
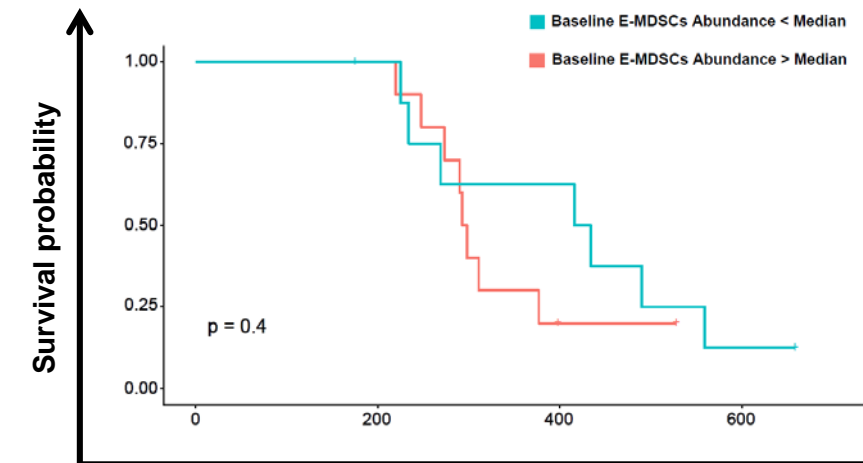
Kaplan-Meier survival curves visualizing OS and PFS among stratum A patients based on the abundance of circulatory MDSC subtypes at baseline.

OS:

E-MDSCs

M-MDSCs

Total MDSCs



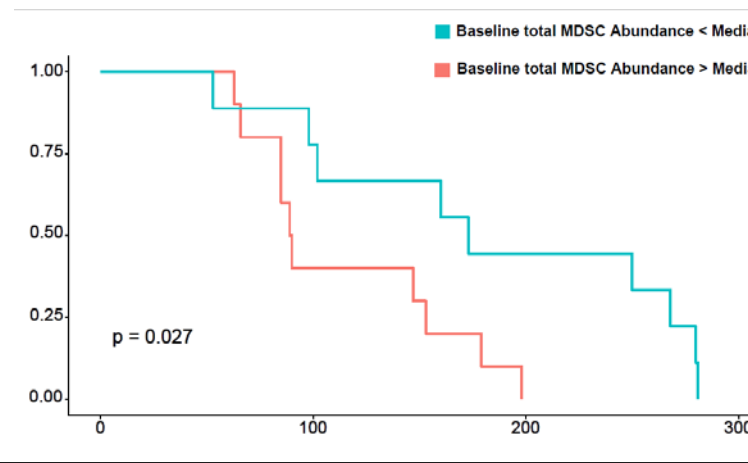
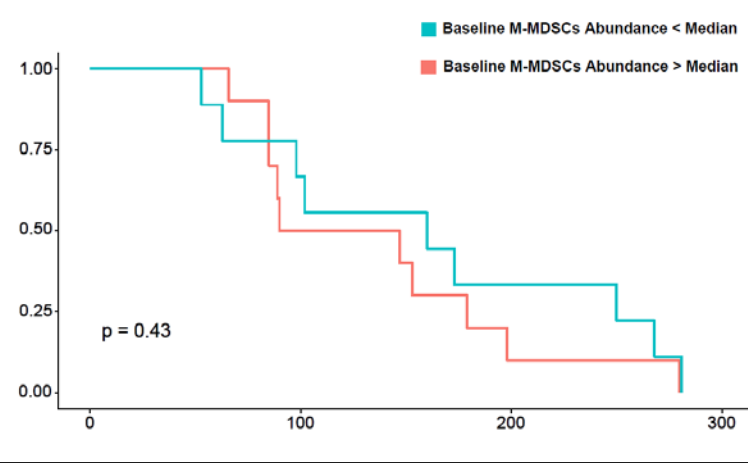
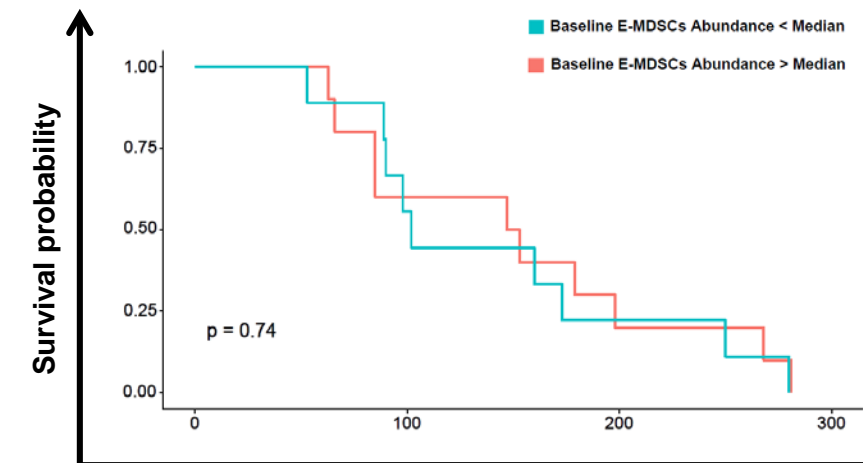
Time (days)

PFS:

E-MDSCs

M-MDSCs

Total MDSCs

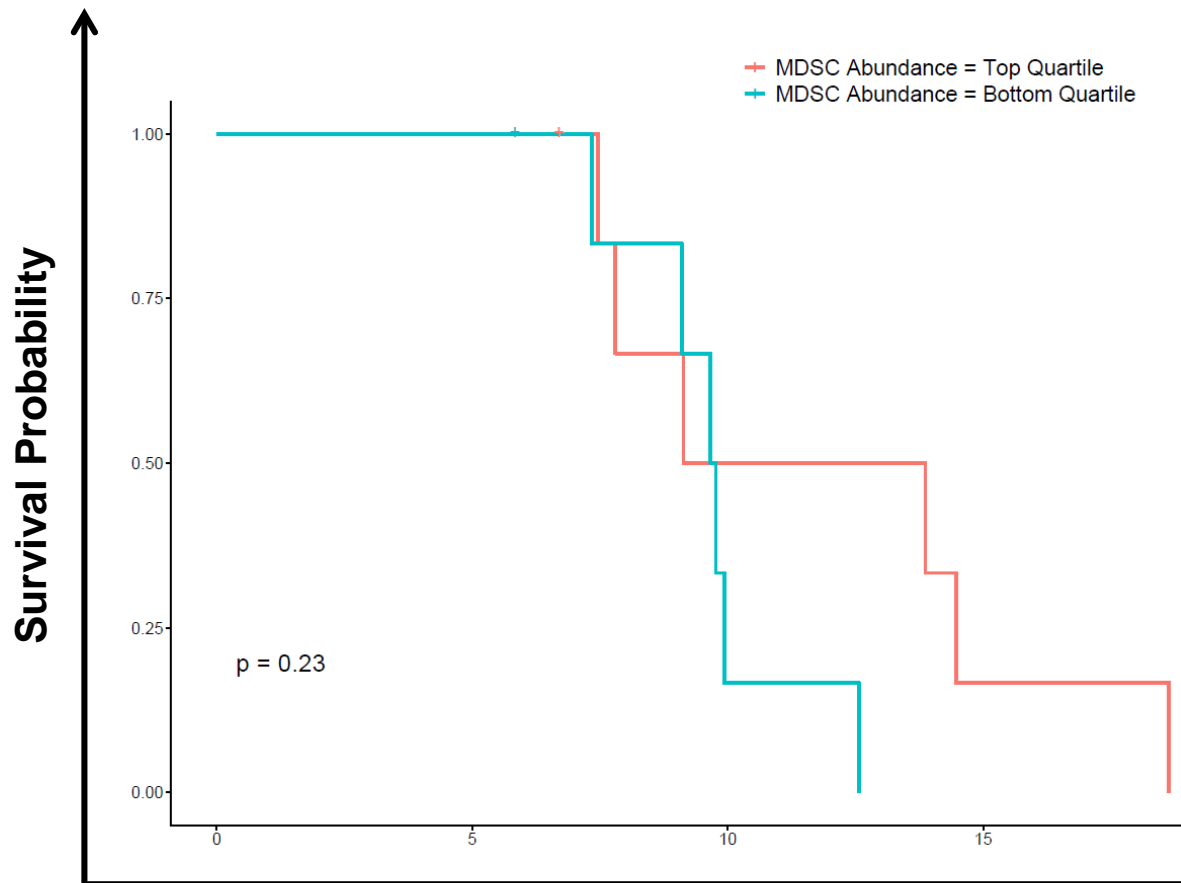


Time (days)

Figure S17

Kaplan-Meier survival curves visualizing OS of strata A+B and stratum A patients with MDSC abundances in upper and lower quartile of their respective cohorts

Strata A + B Patients



Stratum A Patients

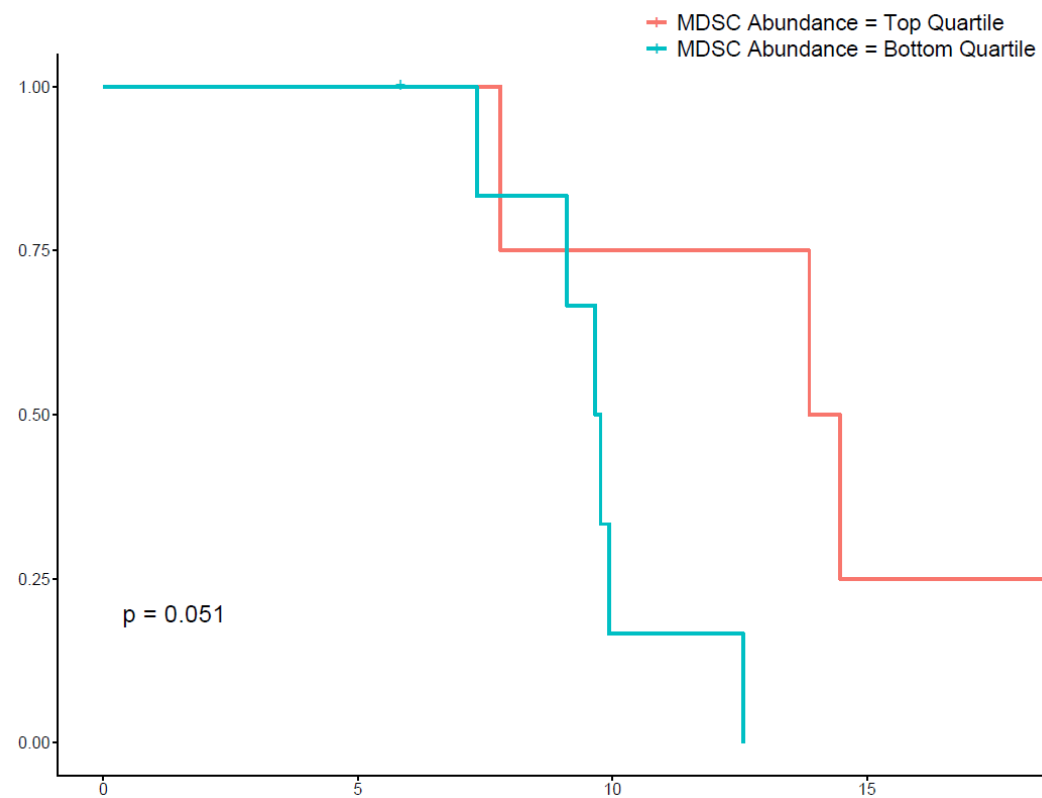
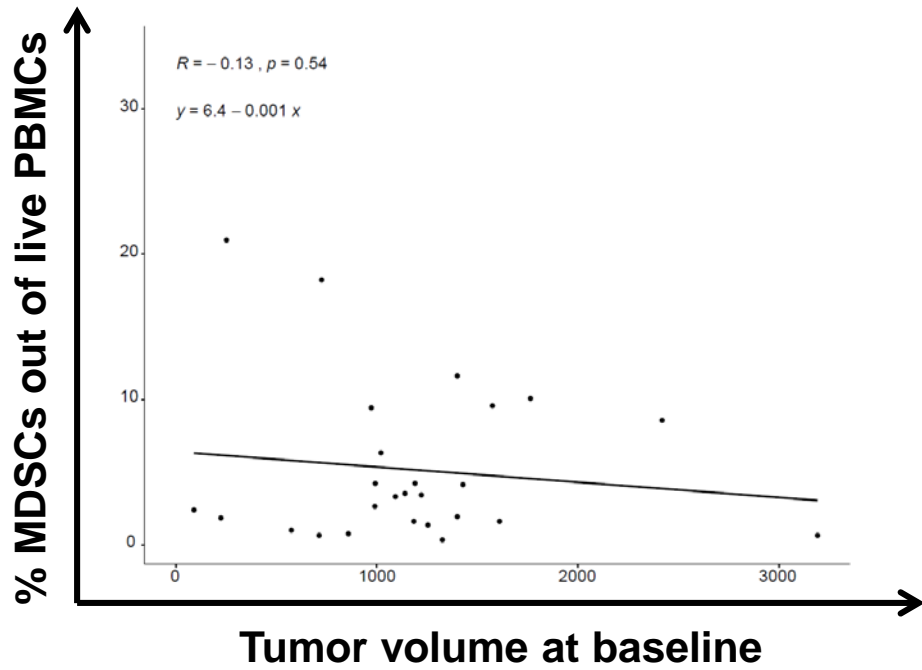


Figure S18

Linear models correlating baseline tumor volume and age with baseline MDSC abundance utilizing Spearman and Pearson correlation methods

Pearson product moment correlation



Spearman rank-order correlation

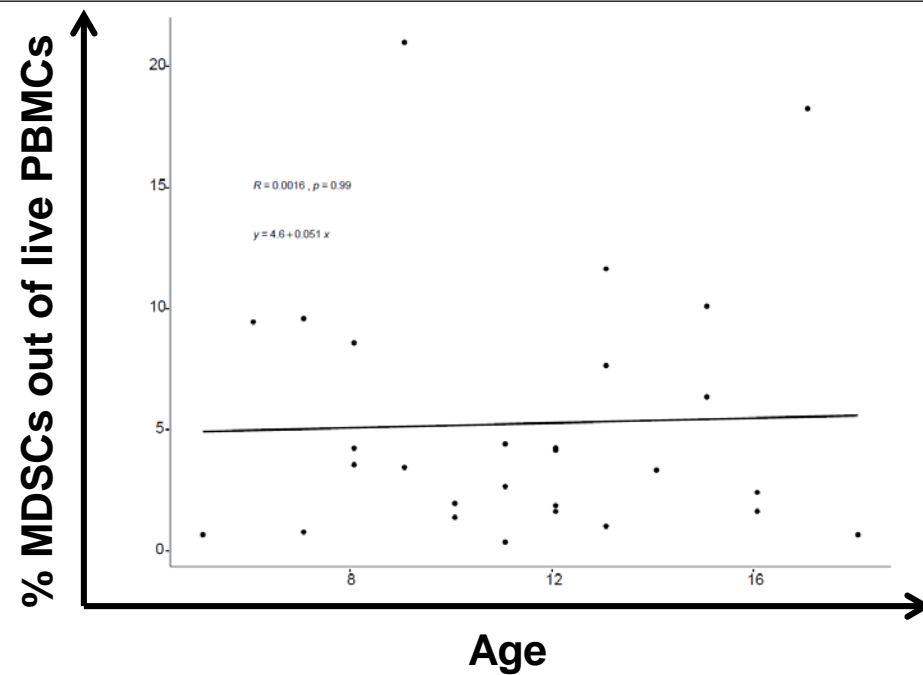
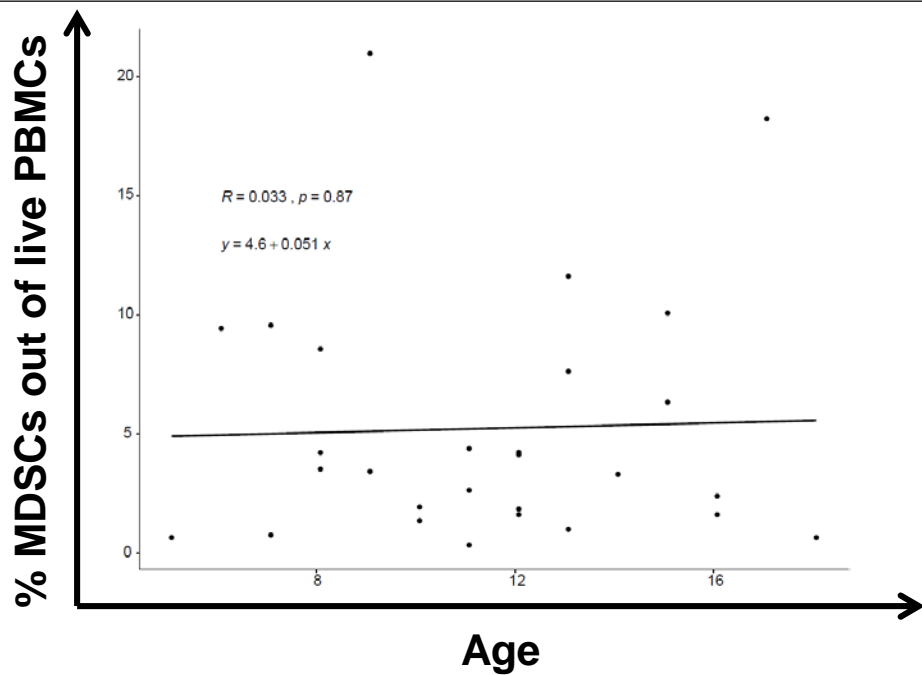
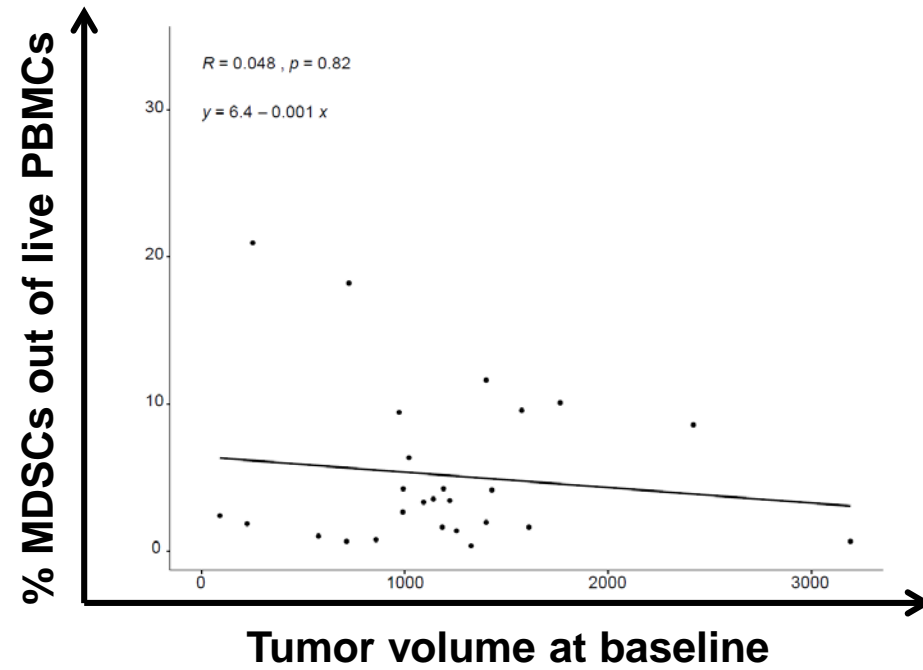
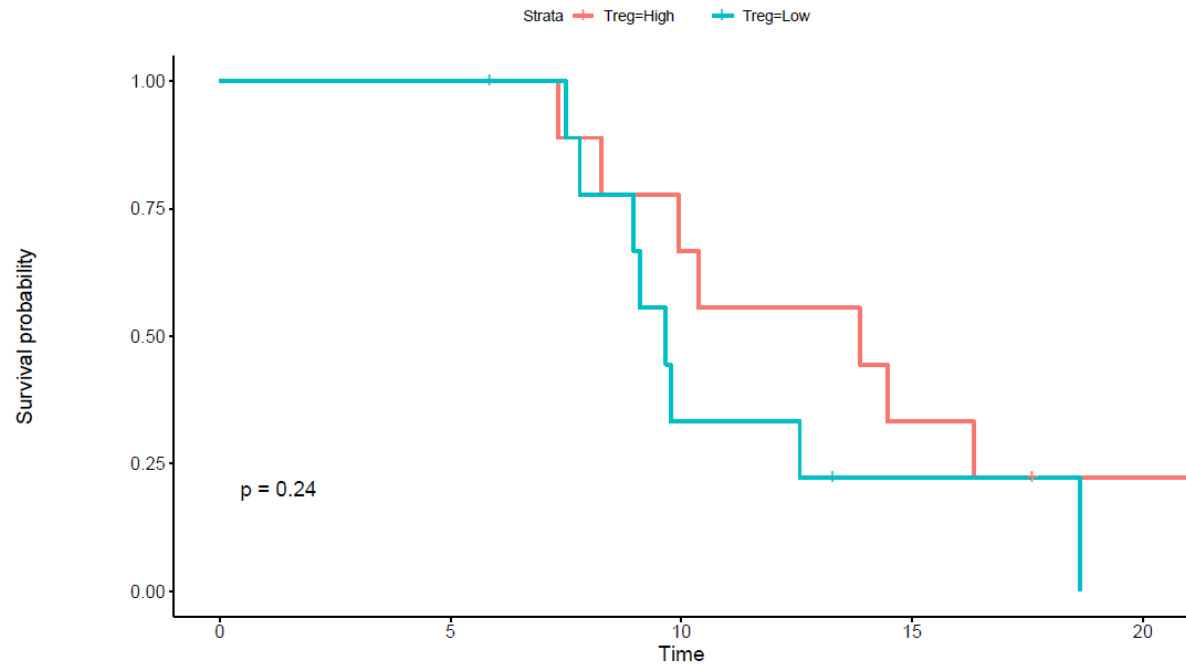


Figure S19

Kaplan-Meier survival curves visualizing OS and PFS of stratum A patients stratified based on Treg abundances above and below median

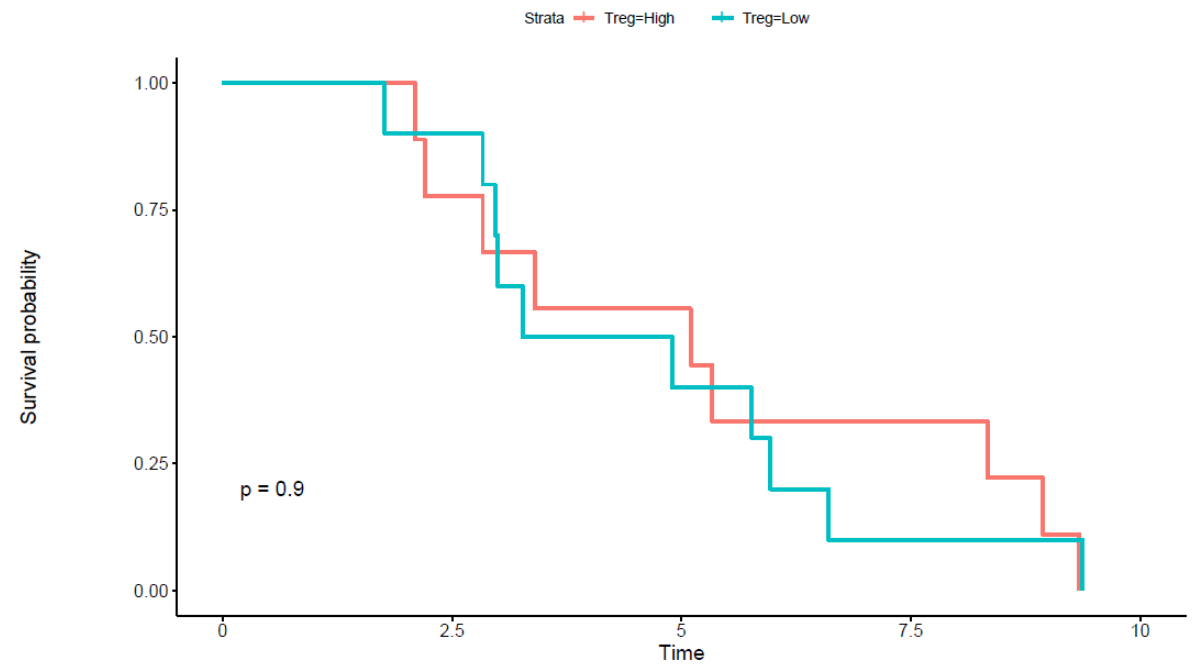
Overall Survival



Number at risk

Strata	Time 0	Time 5	Time 10	Time 15	Time 20
reg.group=High	10	9	6	3	1
reg.group=Low	10	10	3	1	0

Progression-free Survival



Number at risk

Strata	Time 0	Time 2	Time 4	Time 6	Time 8	Time 10
reg.group=High	10	9	5	3	3	0
reg.group=Low	10	9	5	2	1	0

Figure S20

Spider plot depicting longitudinal patient-specific H3.3K27M-reactive CD8+ T-cell frequencies of patients based on dexamethasone administration during vaccine schedule

Patients on steroids (n = 7)

Patients not on steroids (n = 11)

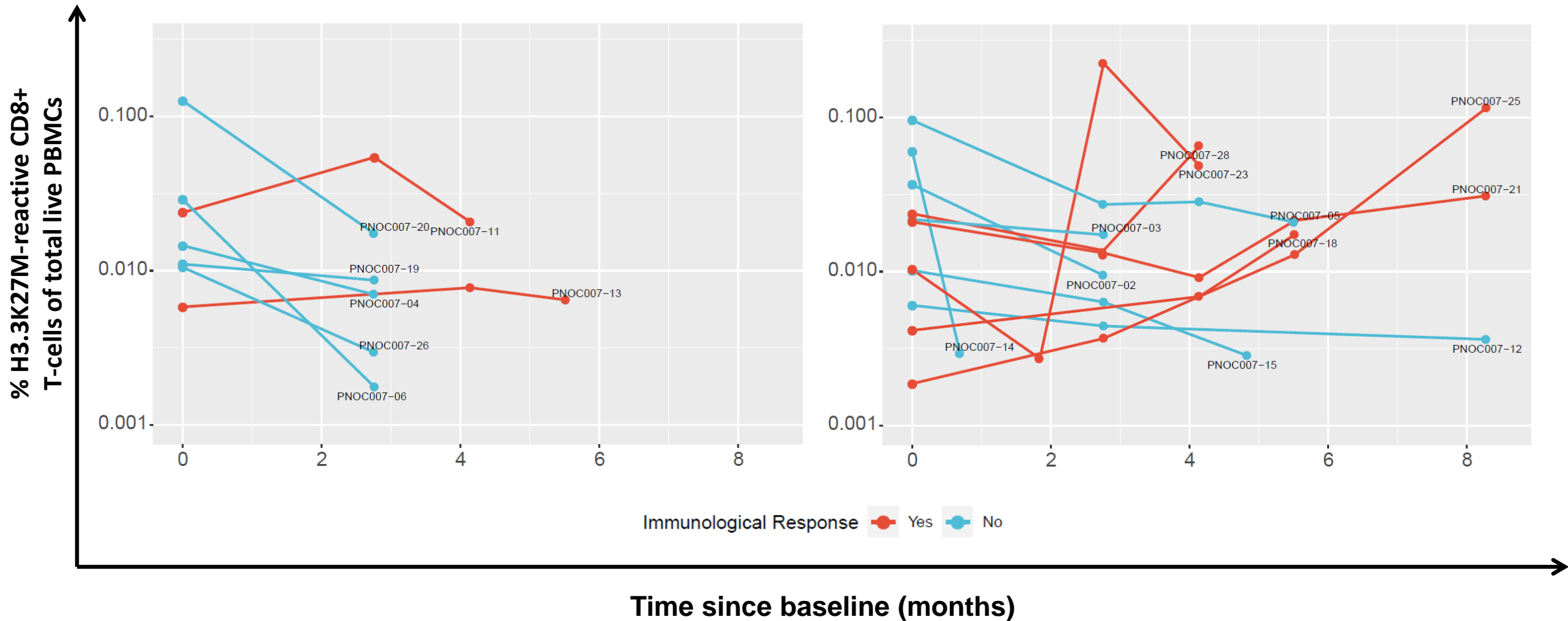


Figure S21

Dexamethasone administration is associated with circulatory MDSC levels and negatively associated with rates of CD8+ T-cell responses and survival in strata A and B patients. *Top left*, waterfall plot depicting the overall levels of circulatory MDSCs at baseline among strata A and B patients. *Bottom left*, boxplot depicting overall levels of circulatory MDSCs at baseline among strata A and B patients. *Top right*, waterfall plot depicting the overall longitudinal percent change of H3.3K27M-reactive CD8+ T-cells at the final time point analyzed relative to baseline for patients treated with dexamethasone pre-treatment (*yellow*), patients receiving dexamethasone after commencement of vaccination (*red*), and patients not receiving dexamethasone on study. (*blue*). *Bottom right*, Kaplan-Meier survival curves visualizing the OS of strata A and B patients based on pre-treatment dexamethasone administration. Cohorts were divided by patients not receiving dexamethasone at baseline (*blue*), patients receiving 1mg doses of dexamethasone (*red*), and patients receiving 2mg doses of dexamethasone (*green*).

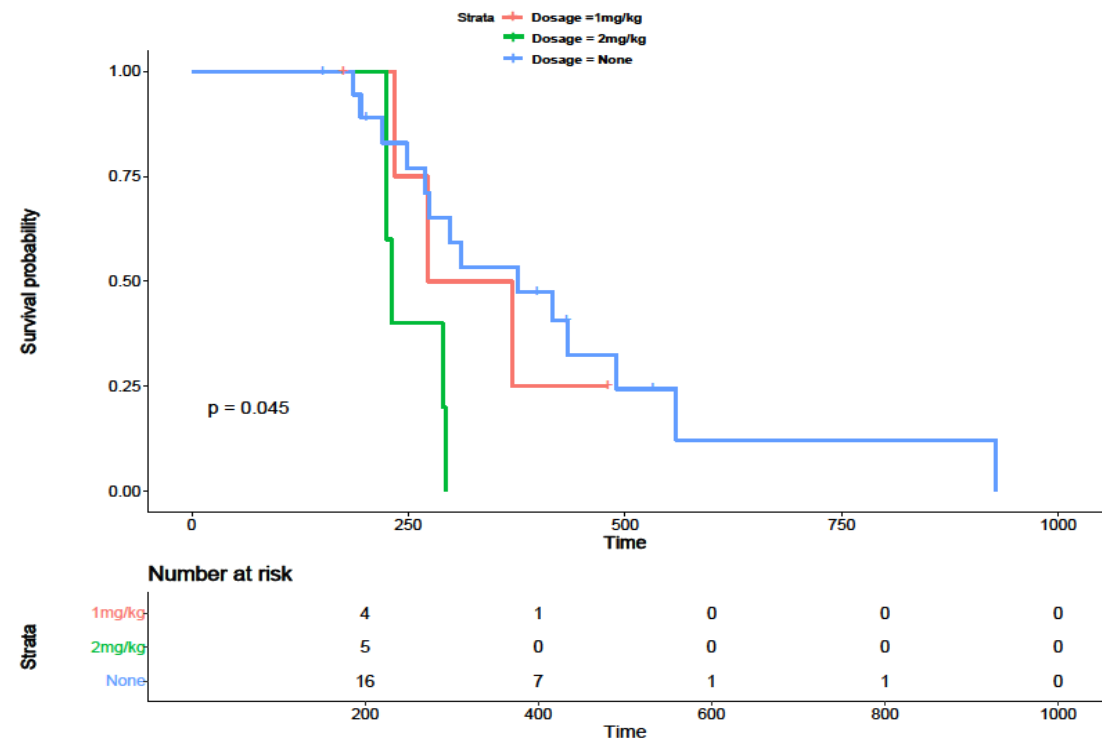
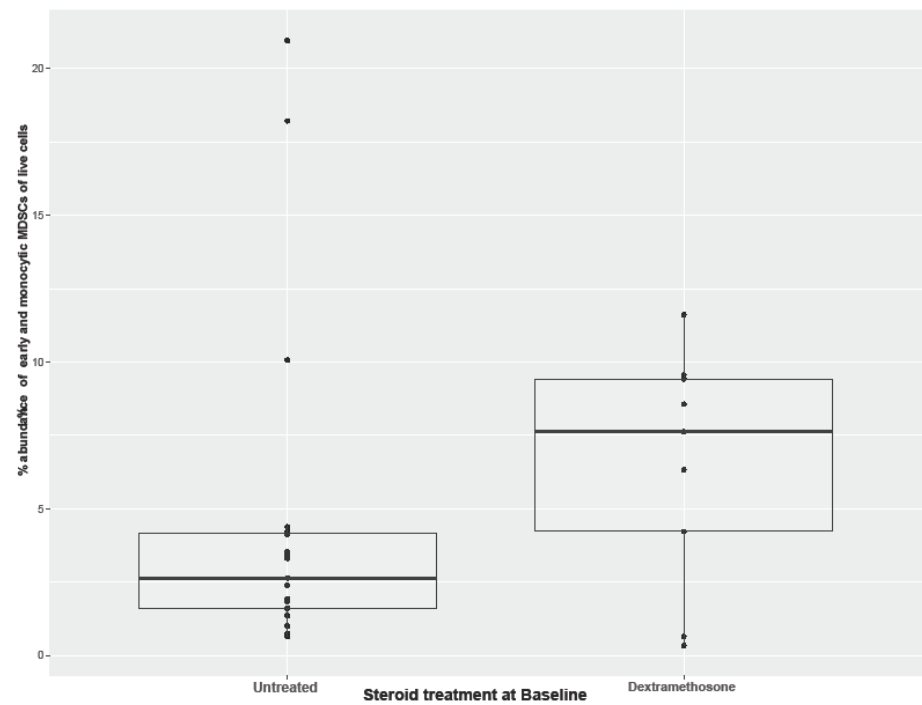
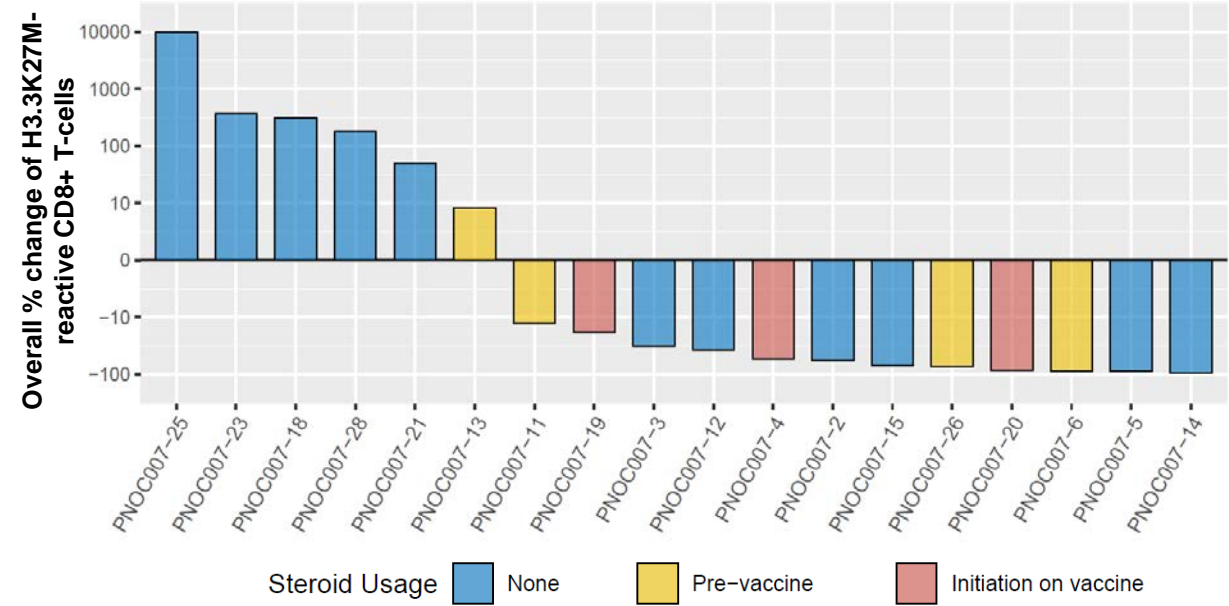
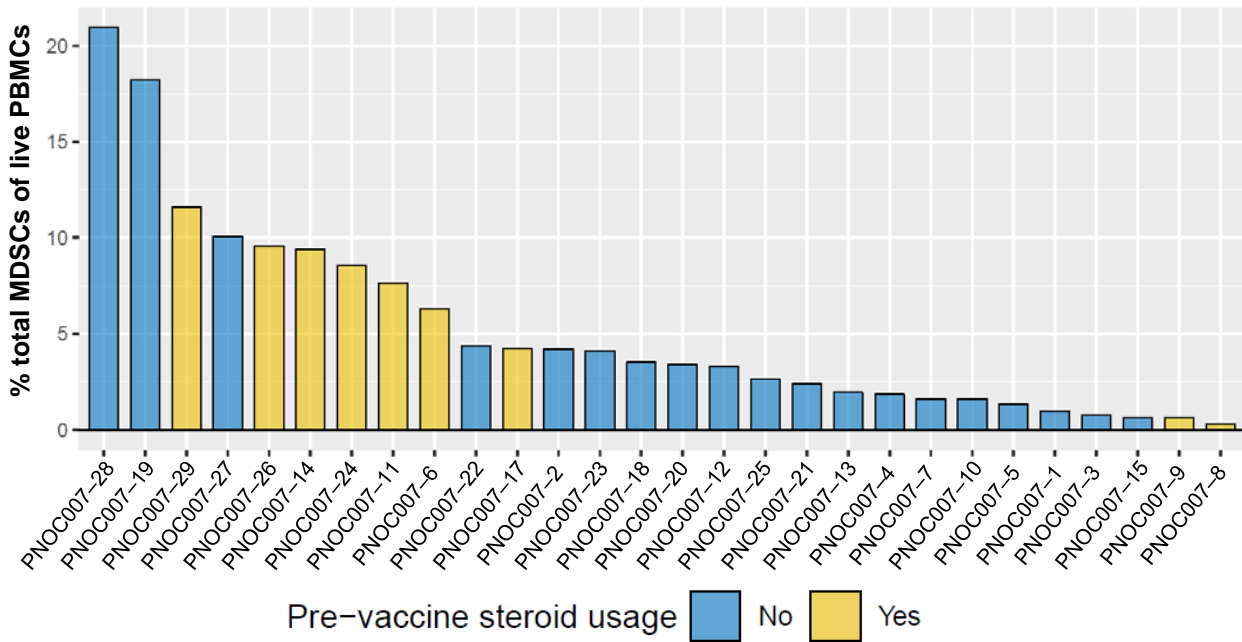


Figure S22

Post-radiation therapy mutation allelic frequency as assessed by liquid biopsy is not predictive of improved patient outcomes. *Left*, plasma ctDNA, defined by H3.3K27M mutation allele frequency (MAF) $\geq 0.001\%$, was detected at baseline (Week 0), in 19 out of 27 patients (70.4%; n=13 Stratum A, n=6 Stratum B). *Right*, Kaplan-Meier survival curves visualizing the OS (top) and PFS (bottom) for patients from which plasma ctDNA was detected at baseline (*red*) compared to patients who did not exhibit plasma ctDNA (*blue*).

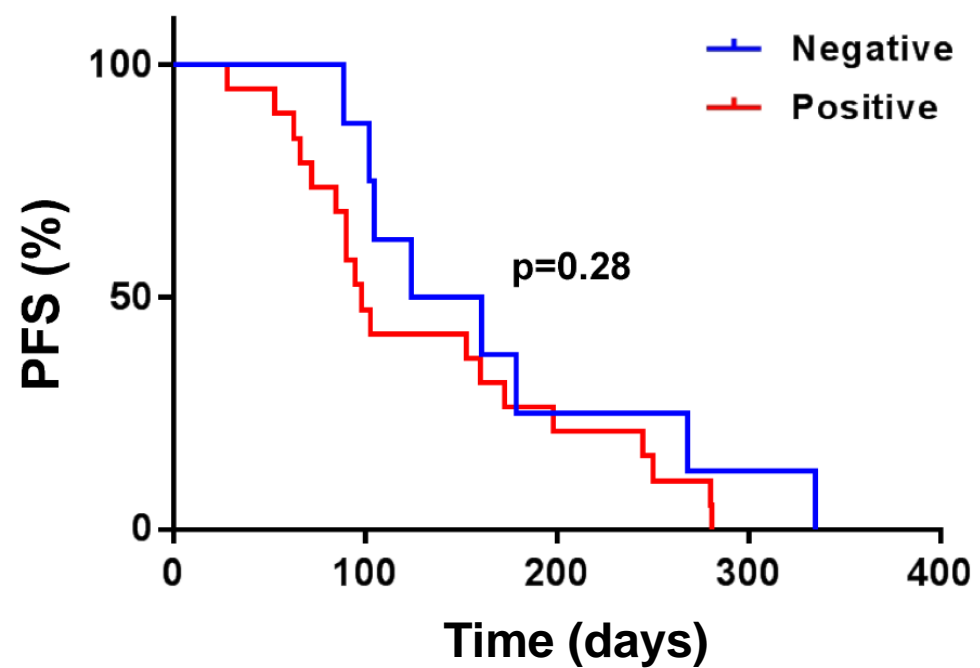
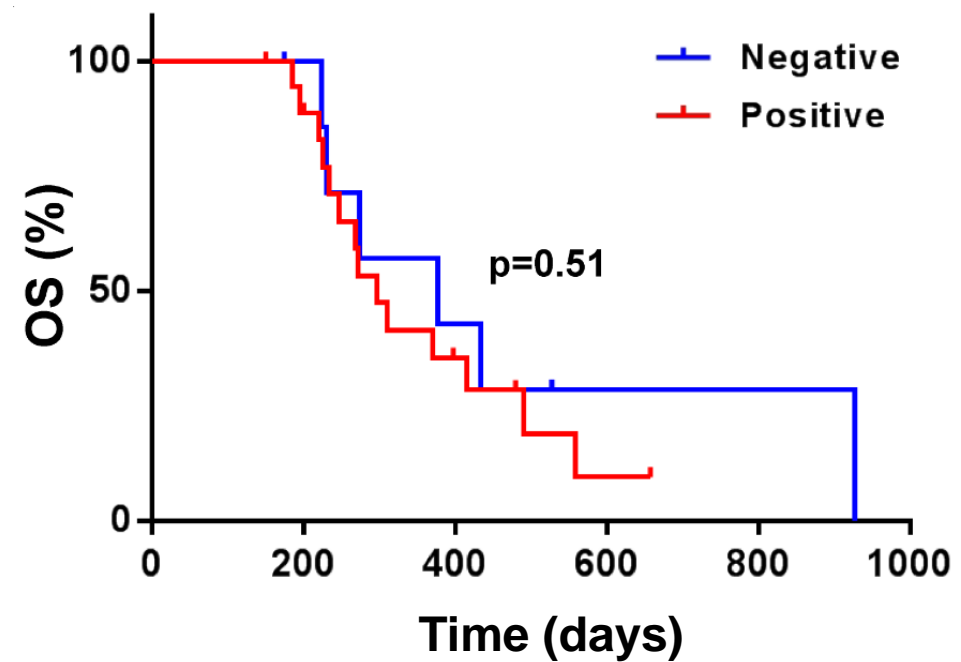
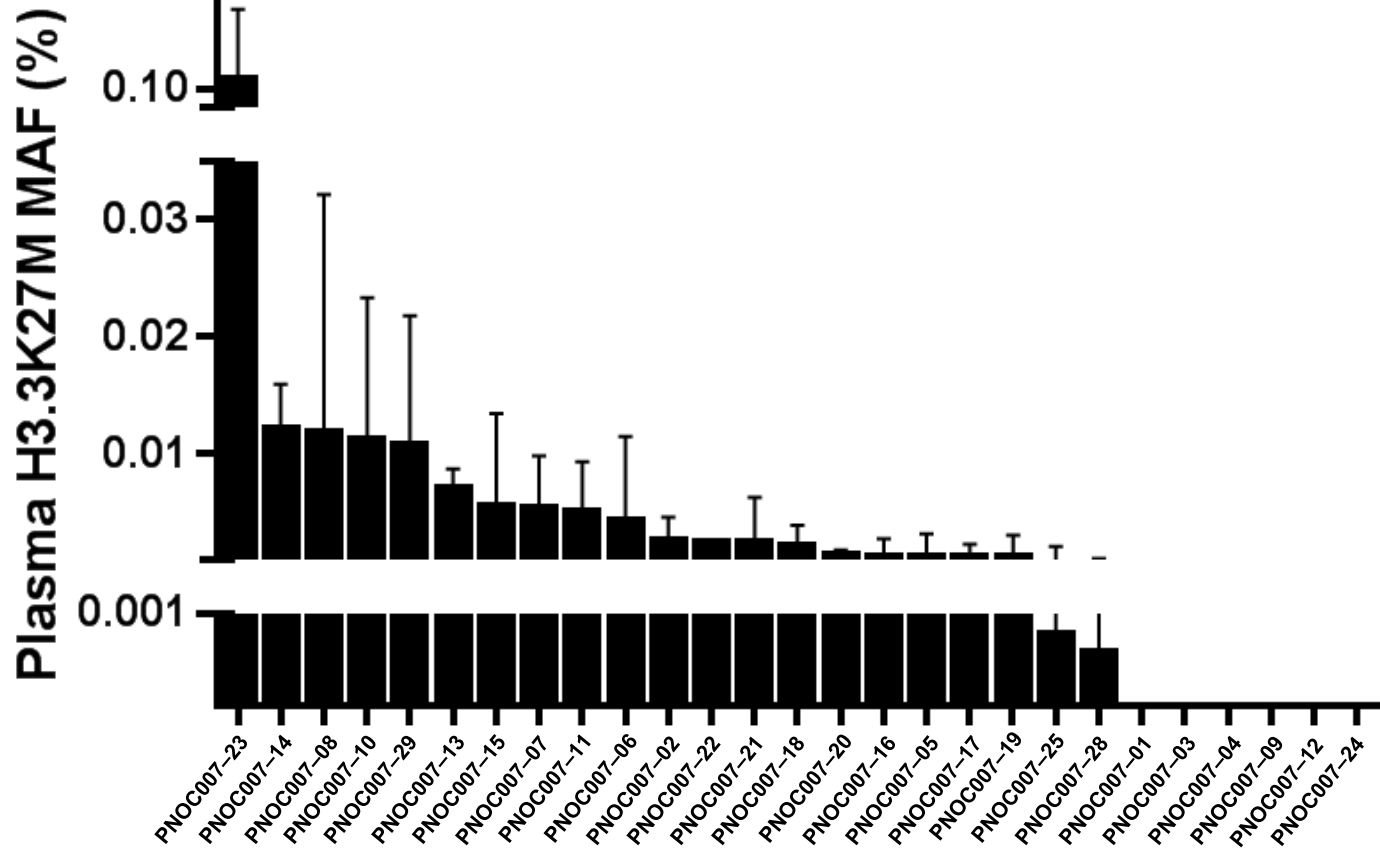


Figure S23

Longitudinal fluctuations in plasma ctDNA do not correlate with patient outcomes. *Left*, longitudinal monitoring of plasma ctDNA indicates changes in ctDNA abundance during the course of therapy, as exemplified by serial ctDNA analysis from six patients (PNOC007-13, -14, -18, -21, -23 and -25). *Right*, Kaplan-Meier curve visualizing the OS of patients exhibiting an increase in plasma ctDNA between baseline and week 12 (*red*) compared to patients who showed a decrease during this time (*blue*).

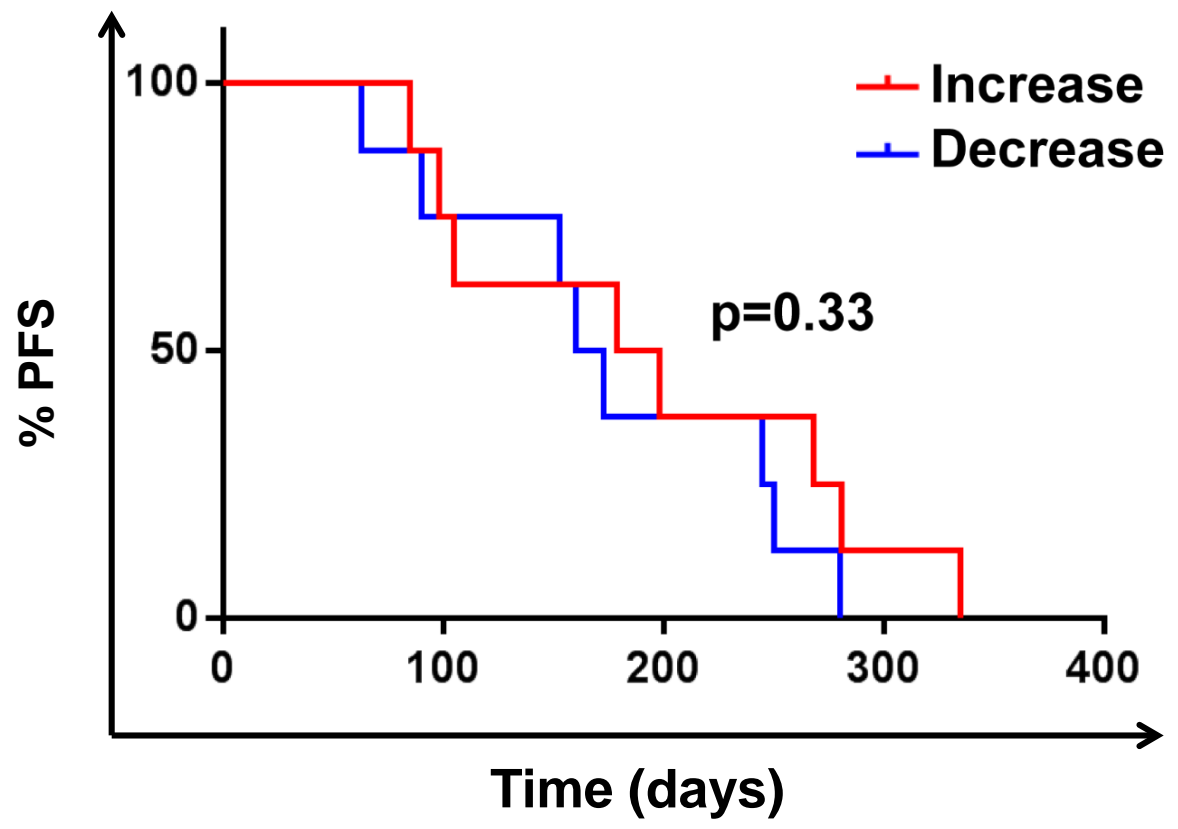
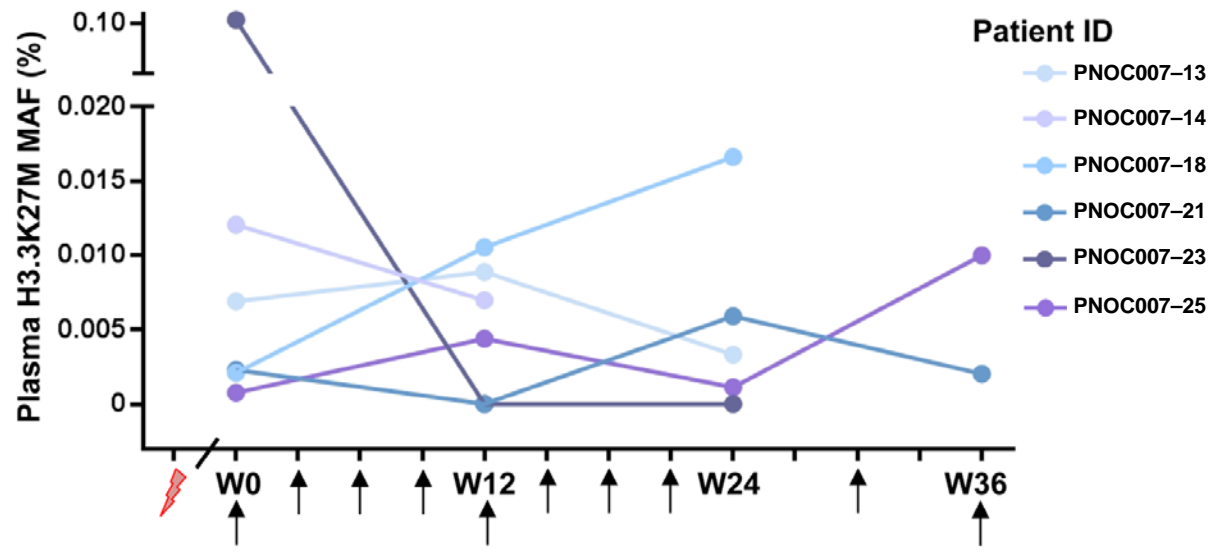
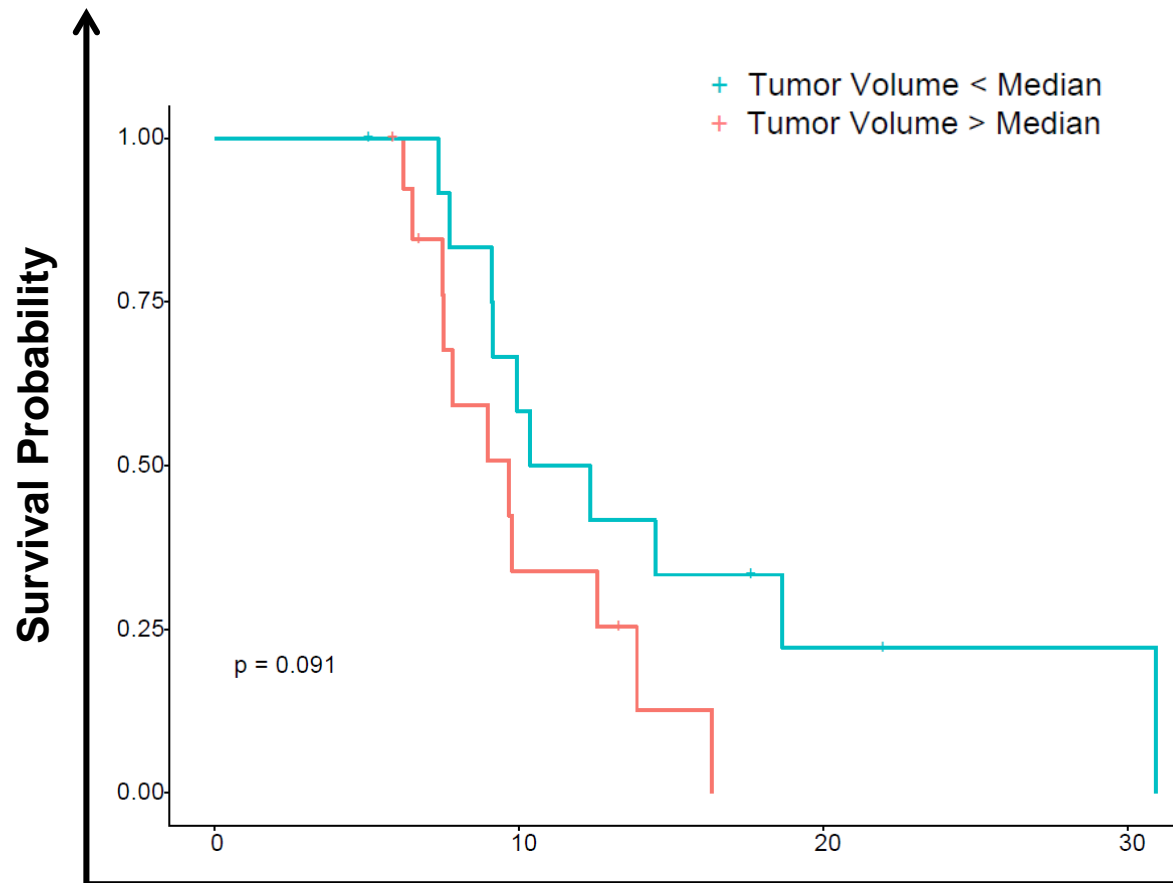


Figure S24

Kaplan-Meier survival curve visualizing OS of patients stratified based on a median threshold of tumor volume at baseline

Strata A + B Patients



Stratum A Patients

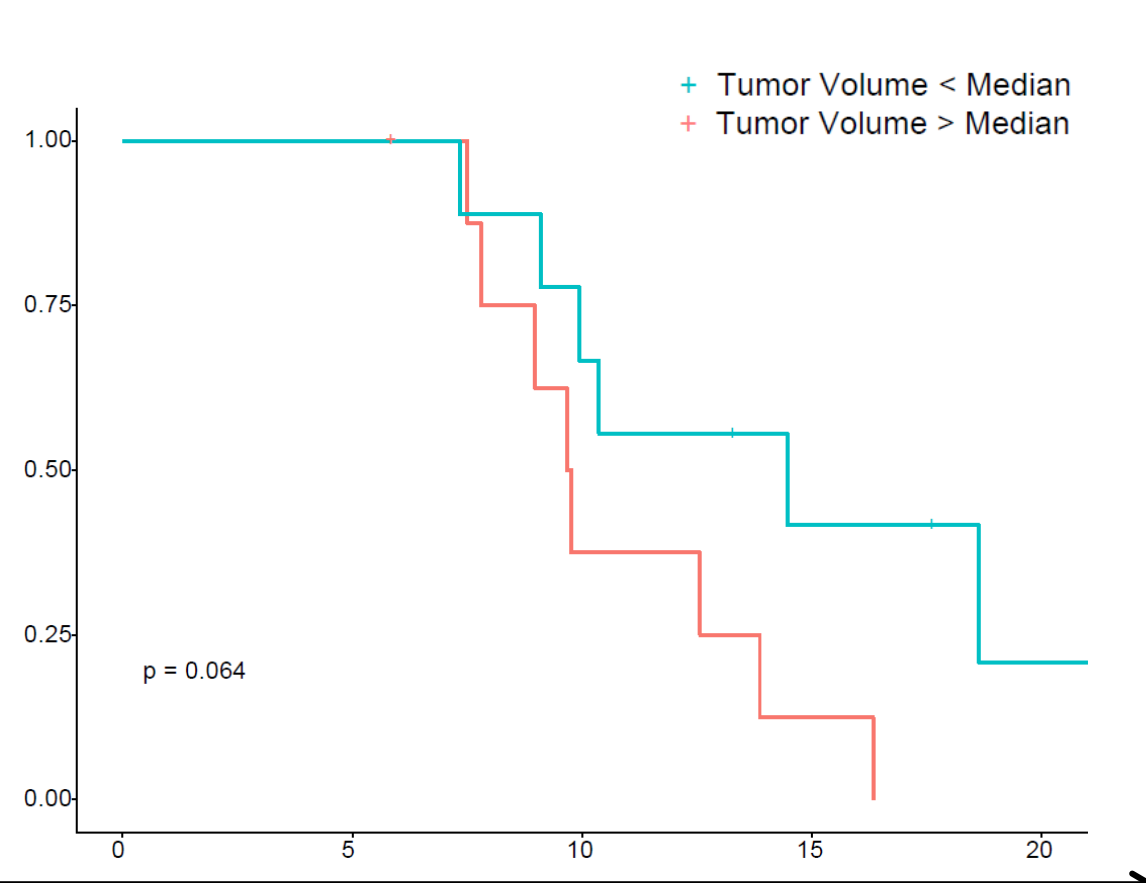
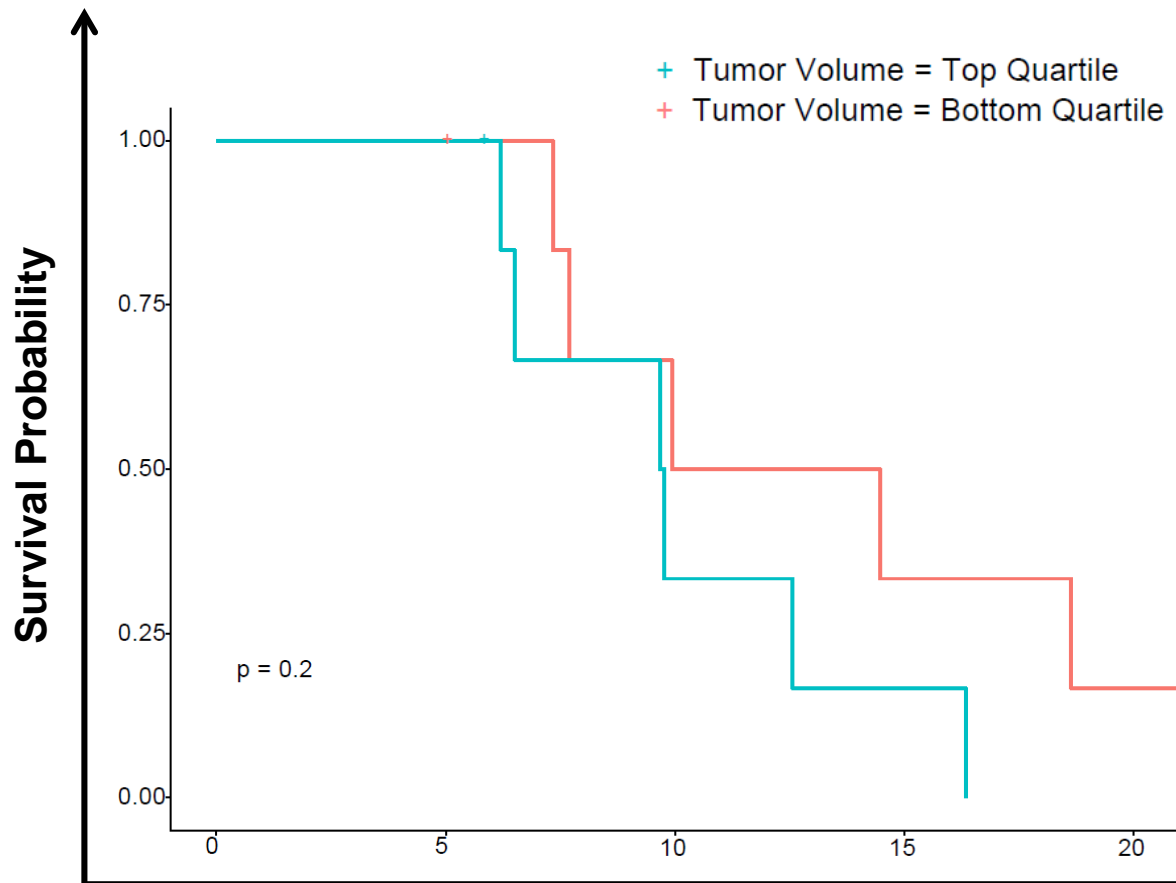


Figure S25

Kaplan-Meier survival curve visualizing OS of patients stratified based on upper and lower quartiles of tumor volume at baseline

Strata A + B Patients



Stratum A Patients

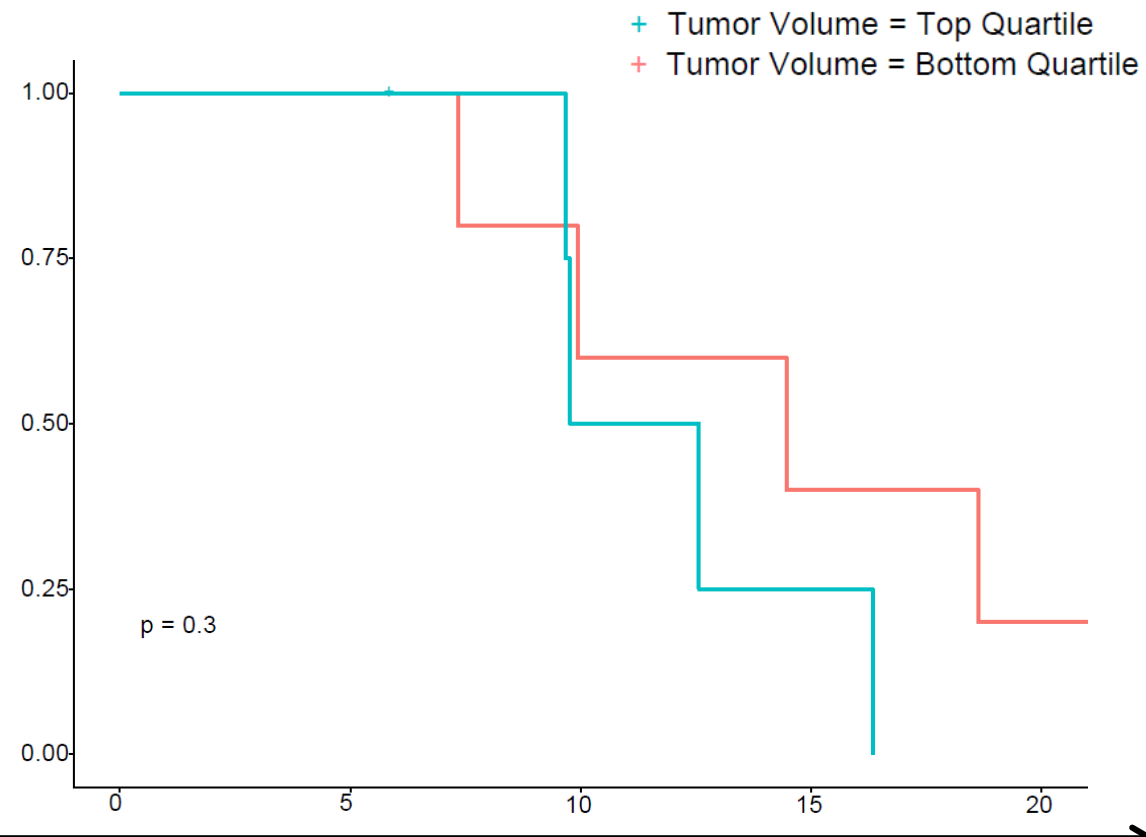
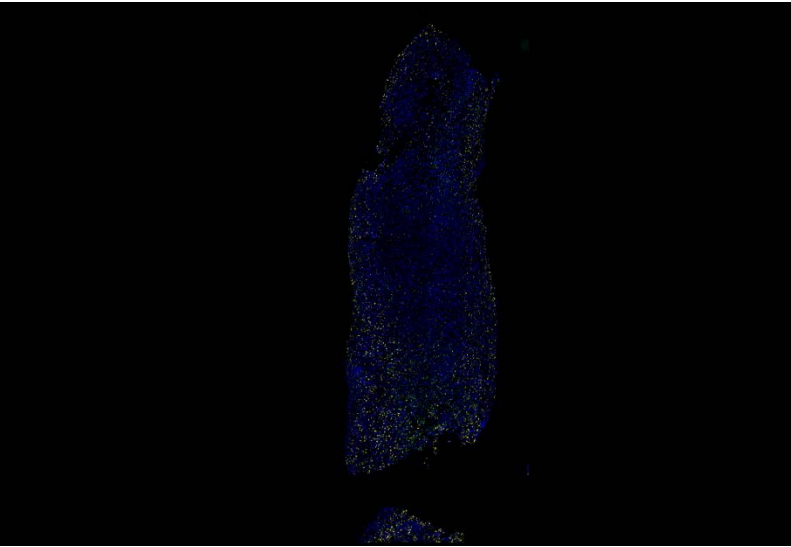
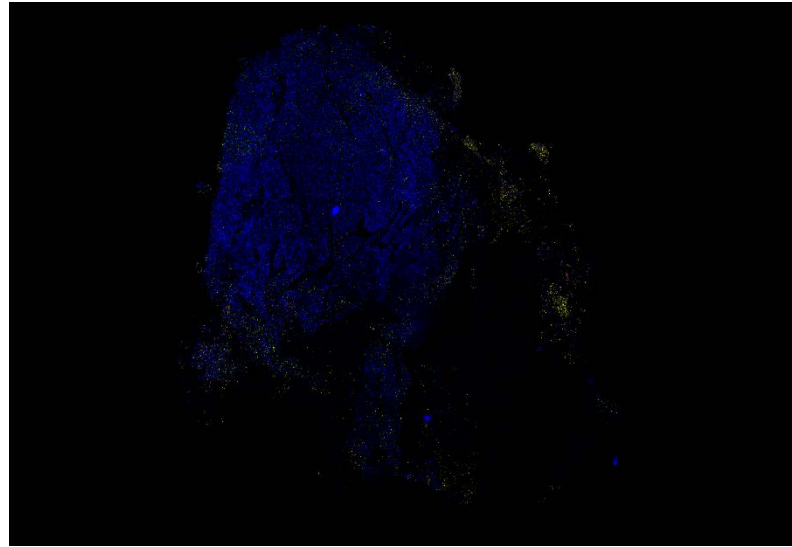
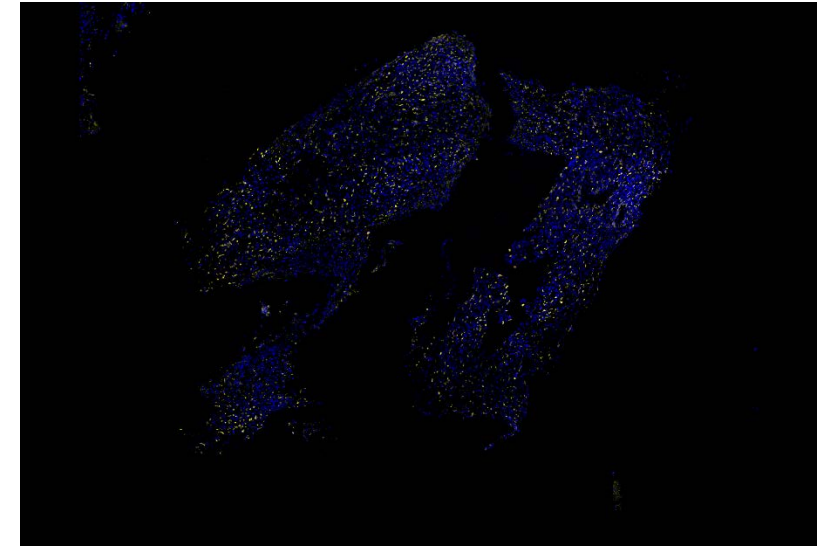


Figure S26

Representative immunofluorescence images quantifying MDSC abundance in tumor microenvironment. Live cells were identified using DAPI nuclear stain. MDSCs were identified using FITC-conjugated Iba1, Cy5-conjugated CD33, and rhodamine-conjugated HLA-DR antibodies. MDSCs were classified as live cells that were Iba1⁺ CD33⁺ HLA-DR^{low}.

PNOC007-05**PNOC007-17****PNOC007-22**

Patient ID	Number of cells analyzed:	% MDSCs of live cells in TME	% MDSCs of live cells in PBMCs
PNOC007-05	4.25e4	0.019%	1.36%
PNOC007-17	6.44e6	0.153%	4.22%
PNOC007-22	4.22e5	0.0047%	4.38%

Figure S27

Corroboratory plot between circulatory MDSCs analyzed on CyTOF and MDSCs identified through immunohistochemistry.

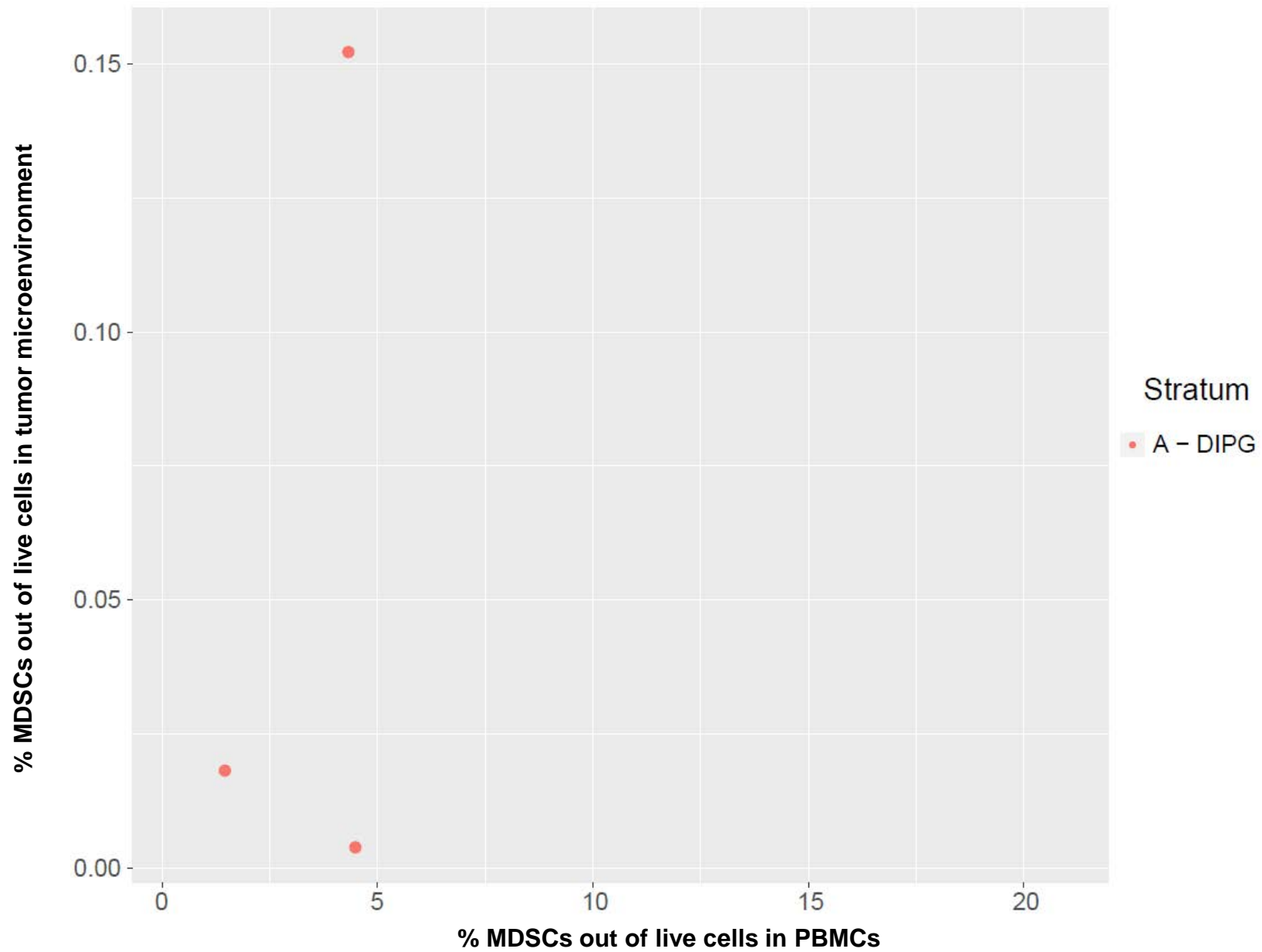
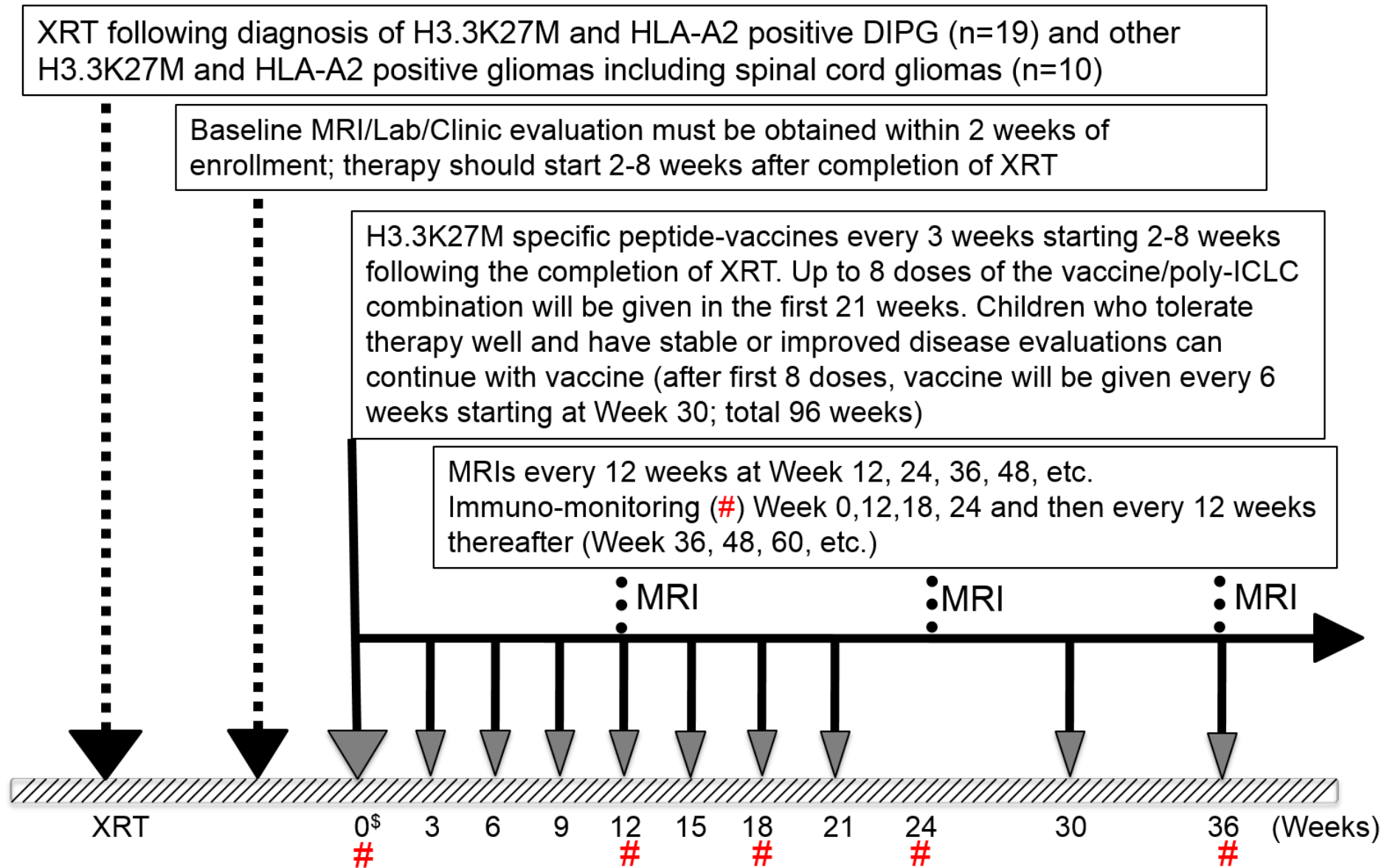


Figure S28

PNOC007 clinical trial therapy schema

Therapy Schema



^{\$}If evidence of radiation induced pseudo-progression on baseline MRI, poly-ICLC administration can be held for up to 12 weeks